NAVAL POSTGRADUATE SCHOOL

Monterey, California

THESIS

ON THE CONSEQUENCES OF BI-MAXWELLIAN DISTRIBUTIONS ON PARALLEL ELECTRIC FIELDS

by

Lewis J. Scott

December, 1991

Thesis Advisor: R. C. Olsen

REPORT DOCUMENTATION PAGE

1a. REPORT SECURITY CLASSIFICATION UNCLASSIFIED	1b. RESTRICTIVE MARKINGS
2a. SECURITY CLASSIFICATION AUTHORITY	3 DISTRIBUTION/AVAILABILITY OF REPORT Approved for public release; distribution is unlimited.
2b. DECLASSIFICATION/DOWNGRADING SCHEDULE	
4. PERFORMING ORGANIZATION REPORT NUMBER(S)	5. MONITORING ORGANIZATION REPORT NUMBER(S)
6a. NAME OF PERFORMING ORGANIZATION Naval Postgraduate School 6b. OFFICE SYMBOL (*If applicable*) CODE 33	7a NAME OF MONITORING ORGANIZATION Naval Postgraduate School
6c. ADDRESS (*City, State, and ZIP Code*) Monterey, CA 93943-5000	7b. ADDRESS (*City, State, and ZIP Code*) Monterey, CA 93943-5000
8a. NAME OF FUNDING/SPONSORING ORGANIZATION 8b. OFFICE SYMBOL (*If applicable*)	9. PROCUREMENT INSTRUMENT IDENTIFICATION NUMBER
8c ADDRESS (*City, State, and ZIP Code*)	10. SOURCE OF FUNDING NUMBERS Program Element No / Project No / Task No / Work Unit Accession Number

11. TITLE (*Include Security Classification*)
ON THE CONSEQUENCES OF BI-MAWELLIAN DISTRIBUTIONS ON PARALLEL ELECTRIC FIELDS

12. PERSONAL AUTHOR(S) Scott, Lewis J.

13a. TYPE OF REPORT	13b. TIME COVERED	14 DATE OF REPORT (*year, month, day*)	15. PAGE COUNT
Master's Thesis	From To	1991, December	78

16. SUPPLEMENTARY NOTATION
The views expressed in this thesis are those of the author and do not reflect the official policy or position of the Department of Defense or the U.S. Government.

17. COSATI CODES			18. SUBJECT TERMS (*continue on reverse if necessary and identify by block number*)
FIELD	GROUP	SUBGROUP	Plasma Physics, Space Physics, Bi-Maxwellian Distributions, Electric Fields, SCATHA, DE-1

19. ABSTRACT (*continue on reverse if necessary and identify by block number*)

Observations made by the SCATHA and DE-1 spacecraft reveal the existence of equatorially trapped plasmas. These plasmas may be described by a bi-Maxwellian distribution function. A resultant parallel electric field arises as a consequence of this distribution function. This thesis models the latitudinal density profiles and the resultant parallel electric field that occurs by integrating the particle distributions to obtain the density, and assuming quasi neutrality to solve for the electric potential and hence the electric field. The results show that the density profile is a maximum at the equator and the equatorially trapped plasma is confined closer to the equator for higher anisotropy ratios. The modeled density profiles are in agreement with some observations. The electric fields that result are on the order of 0.1 uV/m pointing away from the magnetic equator with greater anisotropy leading to larger electric field strength. Density minimums have also been observed at the magnetic equator. This minimum can be explained by the presence of a field aligned electron distribution.

20. DISTRIBUTION/AVAILABILITY OF ABSTRACT	21 ABSTRACT SECURITY CLASSIFICATION	
☒ UNCLASSIFIED/UNLIMITED ☐ SAME AS REPORT ☐ DTIC USERS	UNCLASSIFIED	
22a NAME OF RESPONSIBLE INDIVIDUAL R. C. Olsen	22b TELEPHONE (*Include Area code*) (408) 646-2019	22c OFFICE SYMBOL PH/OS

DD FORM 1473, 84 MAR 83 APR edition may be used until exhausted
All other editions are obsolete

Approved for public release; distribution is unlimited.

ON THE CONSEQUENCES OF BI-MAXWELLIAN DISTRIBUTIONS ON PARALLEL ELECTRIC FIELDS

by

Lewis J. Scott
Lieutenant, United States Navy
B.S., New Mexico State University, 1985

Submitted in partial fulfillment
of the requirements for the degree of

MASTER OF SCIENCE IN PHYSICS

from the

NAVAL POSTGRADUATE SCHOOL
December, 1991

Author: Lewis J. Scott

Approved by: R. C. Olsen, Thesis Advisor

S. Gnanalingam, Second Reader

K. E. Woehler, Chairman
Department of Physics

ABSTRACT

Observations made by the SCATHA and DE-1 spacecraft reveal the existence of equatorially trapped plasmas. These plasmas may be described by a bi-Maxwellian distribution function. A resultant parallel electric field arises as a consequence of this distribution. This thesis models the latitudinal density profiles and the resultant parallel electric field that occurs by integrating the particle distributions to obtain the density, and assuming quasi neutrality to solve for the electric potential and hence the electric field. The results show that the density profile is a maximum at the equator and the equatorially trapped plasma is confined closer to the equator for higher anisotropy ratios. The modeled density profiles are in agreement with some observations. The electric fields that result are on the order of 0.1 μV/m pointing away from the magnetic equator with greater anisotropy leading to larger electric field strength. Density minimums have also been observed at the magnetic equator. This minimum can be explained by the presence of a field aligned electron distribution.

TABLE OF CONTENTS

ACKNOWLEDGEMENT

The author is grateful for support of this work by the Naval Postgraduate School The author would also like to thank R. C. Olsen for his invaluable assistance and my wife Kelly for her support. Thanks to Dr. Don Gurnett, University of Iowa, for DE plasma wave data, from which densities were determined, and Dr. Thomas Moore, NASA/MSFC, for DE/RIMS data.

I. INTRODUCTION

Most of the matter in the universe exists in a plasma state. This is true in the region of space outside the earth's atmosphere. The study of the plasma environment around the earth has practical applications in the understanding of spacecraft charging, and propagation of electromagnetic waves in plasma. Much of our understanding of the earth's environment comes from particle and electromagnetic wave measurements taken by satellites. Such measurements provide basic information on the satellite environment, and clues about basic plasma processes, such as wave-particle interactions. A particularly interesting case of basic plasma physics comes from the geophysical phenomenom known as equatorially trapped plasmas. Equatorially trapped plasmas are those plasmas which are trapped from the magnetic mirror geometry of the earth's magnetic field. These plasmas are typically confined to within a few degrees latitude of the magnetic equator.

The purpose of this thesis is to examine the nature of equatorially trapped distributions. We will show that they may be described by a bi-Maxwellian distribution function, and explore the consequences of this distribution. One consequence of such a distribution is that there will be an electric field parallel to the magnetic field in order to ensure quasi neutrality of the plasma. In the work developed below, self-consistent (equatorial) particle and field distributions will be developed. These results allow mapping of the plasma distribution along the magnetic field line. The density profiles can then be obtained from the integration of the particle distributions. These profiles will be compared to observed density profiles for a comparison between the model and the data

obtained along magnetic field lines. These results will be derived for a steady state plasma where the particles are experiencing motion along a magnetic field line, and the density is low enough so that it may be assumed to be collisionless yet high enough so that a statistical treatment is valid.

Section II of this thesis will present the basic theories of plasma physics which will be used and show examples of plasmas which are equatorially trapped. In Section III, it will be shown that the equatorially trapped plasmas observed by the P78-2 (SCATHA) and Dynamics Explorer-1 (DE-1) satellites may be described by a bi-Maxwellian distribution function. The consequences of this distribution on latitudinal density profiles and resultant parallel electric field will be explored in Section IV.

II. BACKGROUND AND THEORY

A. THEORY

1. Plasma Definition

A plasma is a collection of discrete ionized and neutral particles, which has overall electrical neutrality. The physical dimensions of the plasma must be large in comparison with a characteristic length λ_D called the Debye length. The total number of charges in a sphere with radius λ_D must be much greater than 1.

2. Debye Shielding

The electrostatic potential of a point charge q in a vacuum is given by

$$\psi = \frac{q}{4\pi\varepsilon_0 r} \text{ Volts}$$

where ψ is the electrostatic potential, ε_0 is the permittivity constant ($\varepsilon_0 = 8.85\times10^{-12}$ Farads/m) and r is the distance from the point charge [Ref. 1]. If the charge is immersed in a plasma, a positive charge will attract electrons while repelling ions, and similarly, a negative charge will attract ions and repel electrons. The potential then becomes

$$\psi = \frac{q}{4\pi\varepsilon_0 r} e^{\frac{-r}{\lambda_D}}$$

where

$$\lambda_D \equiv \left[\frac{\varepsilon_0 k T_e}{n e^2}\right]^{1/2}$$

k is the Boltzmann constant ($k = 1.38\times10^{-23}$ Joules/K), T_e is the electron temperature, which is a measure of the average kinetic energy, n is the equilibrium density of the plasma, and e is the charge of electrons ($e = 1.6\times10^{-19}$ Coulombs). This has the effect of screening out electric potentials in a plasma. The electron temperature is used in the definition of λ_D because the electrons are more mobile than the ions and do most of the shielding by creating a surplus or a deficit of negative charge. [Ref. 2]

3. Plasma Parameter

In order for a collection of ionized particles to be considered a collisionless plasma, three conditions must be satisfied. The Debye length must be much less than the dimensions of the plasma. The number of particles in a Debye sphere defined as

$$N_D \equiv \frac{4\pi n \lambda_D^3}{3}$$

must be much greater than 1, that is, there must be a large enough number of particles for Debye shielding to be statistically valid. Finally the frequency of collisions of particles must be low. The plasma paramater g is defined as:

$$g \equiv \frac{1}{N_D}$$

and for a collisionless plasma $g \ll 1$. [Ref 2,3]

Typical values for the plasmasphere, which is the region to be considered in this thesis, are $kT_e =$ 1 eV, $n = 1\times10^6$ m^{-3}, and the typical dimensions are on the order of 1000 km. This gives $\lambda_D \approx 7.4$ m, $N_D \approx 10^9$, and $g \approx 10^{-9}$. Thus the particles considered may be treated as a collisionless plasma.

4. Motion in a Uniform Magnetic Field

A collisionless plasma will behave as a collection of individual particles. The individual charged particles will move in trajectories determined by the applied electric and magnetic fields. For space applications the fields resulting from the particle motion are often small and may be neglected. This is particularly true for the magnetic field, less so for the electric field. The force acting on a charged particle moving in a combined $\vec{E}$ and $\vec{B}$ field is given by the Lorentz equation:

$$\vec{F} = q(\vec{E} = \vec{v}\times\vec{B})$$

where $\vec{F}$ is the Lorentz force, and $\vec{v}$ is the particle velocity.

For the case where $\vec{E} = 0$, and the magnetic field is uniform, a charged particle will execute simple cyclotron gyration with a frequency

$$\omega_c = \frac{|q|B}{m}$$

and radius

$$r_L \equiv \frac{v_{perp}}{\omega_c} = \frac{mv_{perp}}{|q|B} = \frac{mv\sin\alpha}{|q|B}$$

where m and v are the mass and velocity of the charged particle and the pitch angle α is the angle between the velocity vector of the particle and the magnetic field. The velocity parallel to the magnetic field line, $v_{par} = v\cos\alpha$, is not affected by the magnetic field. This motion describes a circular orbit about a guiding center which is travelling along the magnetic field line with velocity v_{par}. The trajectory of this particle is a helix with it's axis parallel to the field line. [Ref. 3]

5. Magnetic Mirror

The magnetic moment of a gyrating particle is defined to be

$$\mu = \frac{mv_{perp}^2}{2B}.$$

If we now consider a particle gyrating into a slowly converging magnetic field, the magnetic force will have two components. One component is in the plane of the orbit about the guiding center, and the other is along the the field line pointing in the direction of lower B. As the particle travels along the field line, μ remains invariant. Thus as the particle travels from a weak to a strong B field region v_{perp} must increase. Since the total energy must also remain constant, the parallel component of velocity must then decrease. If the magnetic field becomes strong enough v_{par} will become zero and the particle will be reflected back. Thus a particle may become trapped in a magnetic mirror where there is a stronger magnetic field region on either side of a weak field region.

6. Geomagnetic Field

The geomagnetic field may be represented as a magnetic dipole fixed at the center of the earth. The strength of the magnetic field is given by

$$B = \frac{\mu_0 M}{4\pi r^3}(1 + 3\sin^2\lambda)^{1/2}$$

where u_0 is the permeability constant, M is the magnetic dipole moment of the earth, λ is the geomagnetic latitude and r is the distance from the center of the earth. The equation of the field lines is

$$r = r_0\cos^2\lambda = LR_E\cos^2\lambda$$

where R_E is the radius of the earth, and L is a label for a field line, equal to the distance, in earth radii, at which that field line crosses the magnetic equator.

Figure 1 is a schematic representation of the magnetic field lines [Ref. 2]. If we now define the strength of the magnetic field at the equator to be

$$B_0 \equiv \frac{\mu_0 M}{4\pi (LR_E)^3}$$

the strength of the magnetic field is then given by

$$B = \frac{B_0(1 + 3\sin^2\lambda)^{1/2}}{\cos^6\lambda}.$$

The magnetic field of the earth, which is stronger at the poles than at the equator forms a natural magnetic mirror. The distance s along the magnetic field line, defined to be 0 at the equator, is related to the magnetic latitude by

$$s = LR_E\left[\frac{\sin\lambda(1 + 3\sin^2\lambda)^{1/2}}{2} + \frac{\sinh^{-1}(\sqrt{3}\sin\lambda)}{2\sqrt{3}}\right].$$

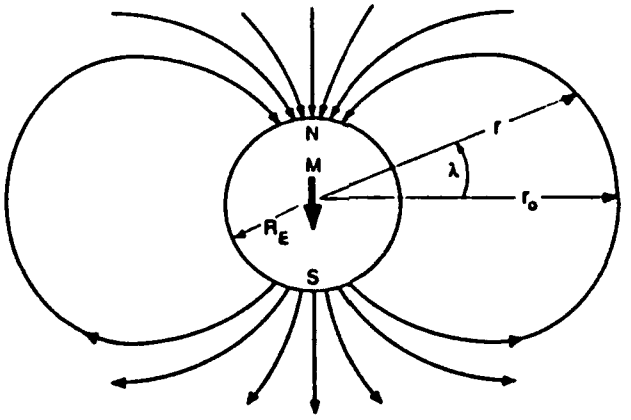

Figure 1. Magnetic Field lines for a dipole [Ref. 2].

7. Statistical Distribution

When dealing with a system which is composed of a very large number of individual particles it becomes impractical to solve the equations of

motion for the system. Instead the particles may be treated statistically through the use of the distribution function. Classically the distribution function gives the probability distribution of the values of the coordinates and momenta of the particles. The density of particles in coordinate space is obtained by integrating the distribution function over momentum or velocity space. That is:

$$n = \int f(\vec{r},\vec{v})d^3\vec{v}$$

where n is the density, and $f(\vec{r},\vec{v})$ is the distribution as a function of position and velocity integrated over three dimensional velocity space.

The two distribution functions of interest in this thesis are the bi-Maxwellian, and the Maxwellian or isotropic distribution functions, given by

$$f_{bi} = n\left[\frac{m}{2\pi kT_{perp}}\right]\left[\frac{m}{2\pi kT_{par}}\right]^{1/2} e^{-\frac{m}{2}\left[\frac{v_{perp}^2}{kT_{perp}}+\frac{v_{par}^2}{kT_{par}}\right]}$$

$$f_{iso} = n\left[\frac{m}{2\pi kT}\right]^{3/2} e^{-\frac{mv^2}{2kT}}$$

where T_{perp} and T_{par} are the characterictic temperatures in the perpencicular and parallel directions with respect to the magnetic field line.

B. PREVIOUS OBSERVATIONS

Observations made by the P78-2 (SCATHA) and the Dynamics Explorer-1 (DE-1) spacecraft at the earth's magnetic equator reveal the existence of equatorially trapped plasmas. A description of the spacecraft instrumentation and environment along with several examples of observed distributions are presented here.

1. P78-2 (SCATHA)

The SCATHA spacecraft was launched in January of 1979 in a near synchronous, near earth orbit. The body of the satellite is cylindrical in shape with a length and diameter of approximately 1.75 meters. The spin rate of the satellite is approximately 1 rpm with an axis perpendicular to the earth-sun line and in the orbital plane. The observations discussed here were taken from the UCSD SC-9 Auroral particles experiment shown in relationship to the SCATHA spacecraft in Figure 2.

The SC-9 experiment consists of 5 Electrostatic Analyzers (ESA's), four of which are contained in two Rotating Detector Assemblies (RDA's). Each RDA contains a pair of ion and electron ESA's, and can be rotated through 220 degrees providing measurements of particle flux at various angles. The fifth ESA, for detecting ions, is mounted in the Fixed Detector Assembly (FDA). The configuration of the SC-9 experiment is shown in Figure 3 [Ref. 4]. One RDA is a high energy (HI) detector covering an energy range from 1 eV to 81 keV. The other RDA (LO detector) and the FDA (FIX detector) are low energy detectors covering an energy range from 1 eV to 2 keV. These detectors scan the energy range in 64 exponentially spaced energy levels over a period of 16 seconds, with an option to dwell at specific energy levels from 2 to 128 seconds. The energy resolution at each step is approximately 20 percent. [Ref. 4,5]

On day 179 of 1979 the LO detector was parked parallel to the spin axis of the satellite, and the HI and FIX detectors were looking in the radial direction. The HI and FIX detectors provide pitch angle distributions, while the LO detector, which is looking approximately perpendicular to the magnetic field line was used to provide energy distribution information. Figures 4 and 5 show

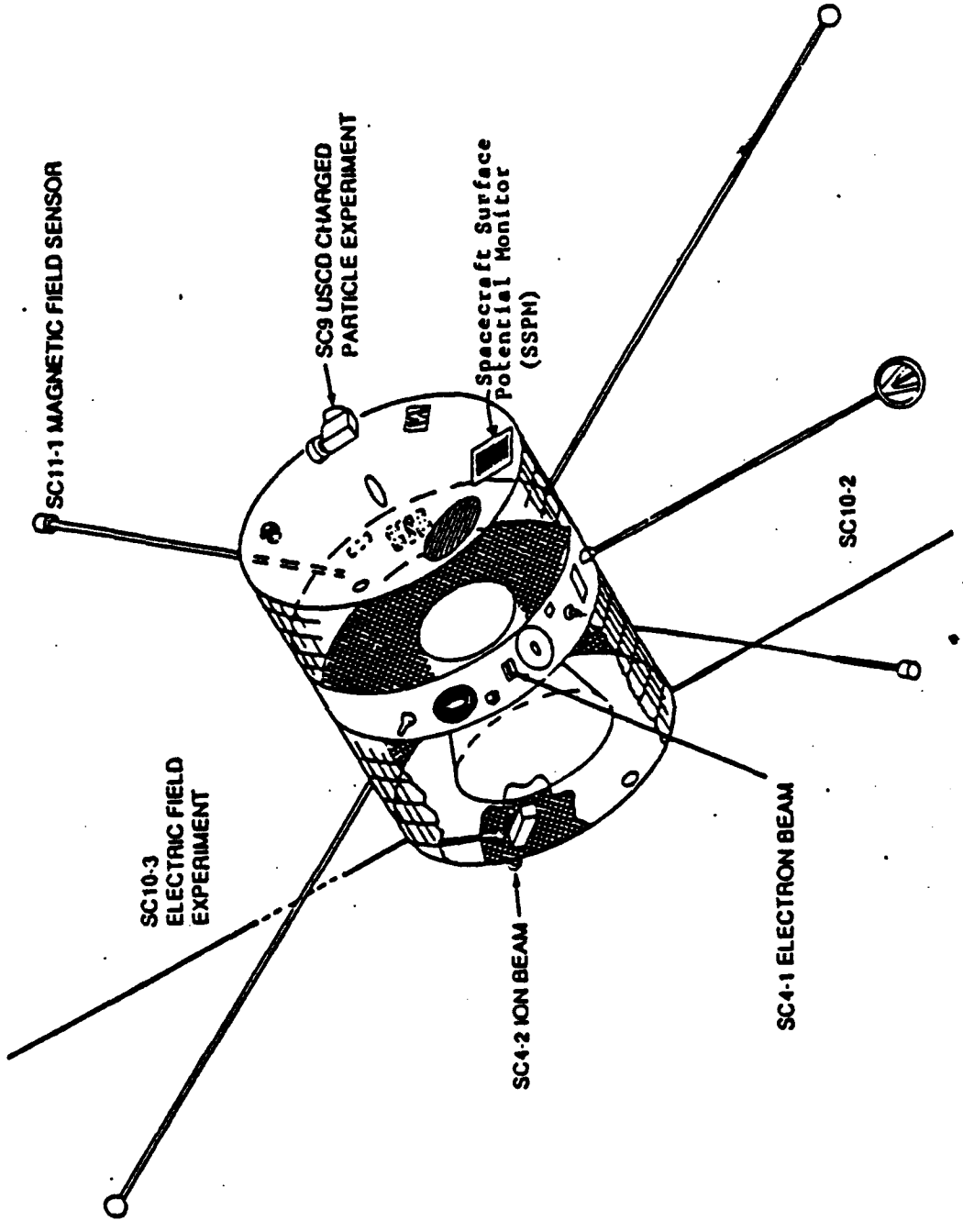

Figure 2. SC-9 Auroral particles experiment on P78-2 SCATHA spacecraft. [Ref. 4]

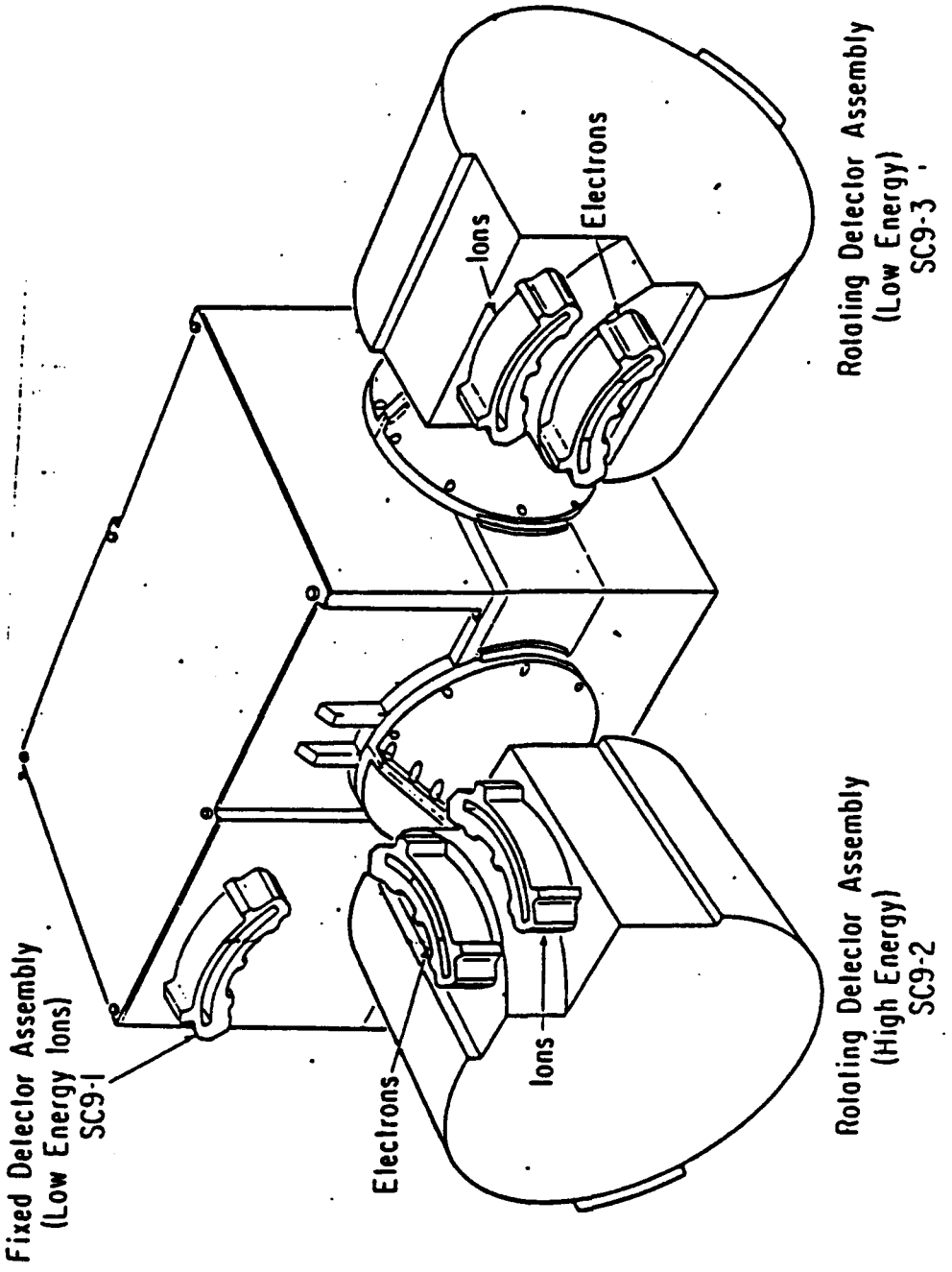

Figure 3. SC-9 Auroral Particles experiment. [Ref. 4]

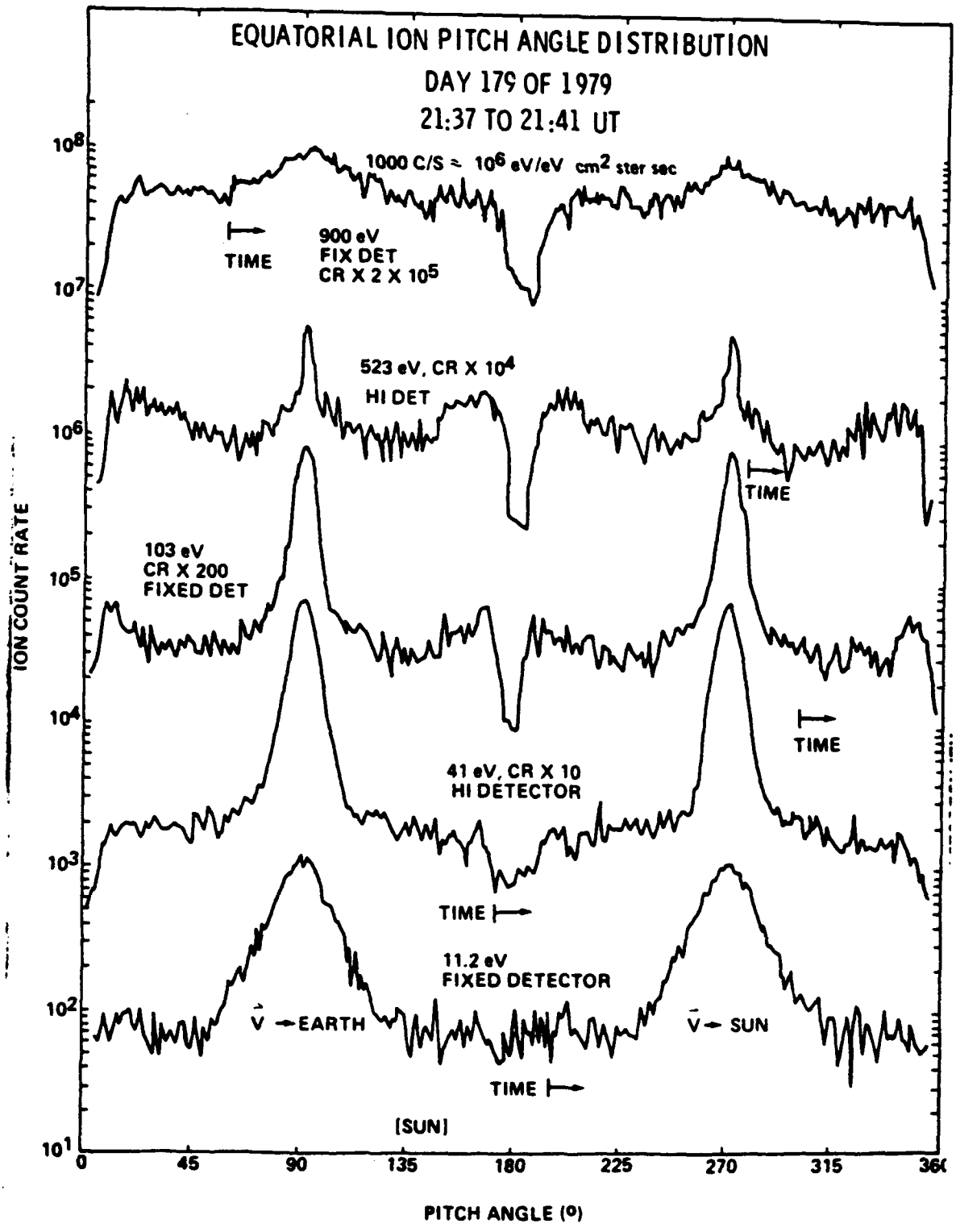

Figure 4. Ion Pitch Angle Distribution, SCATHA Day 179 of 1979. [Ref. 5]

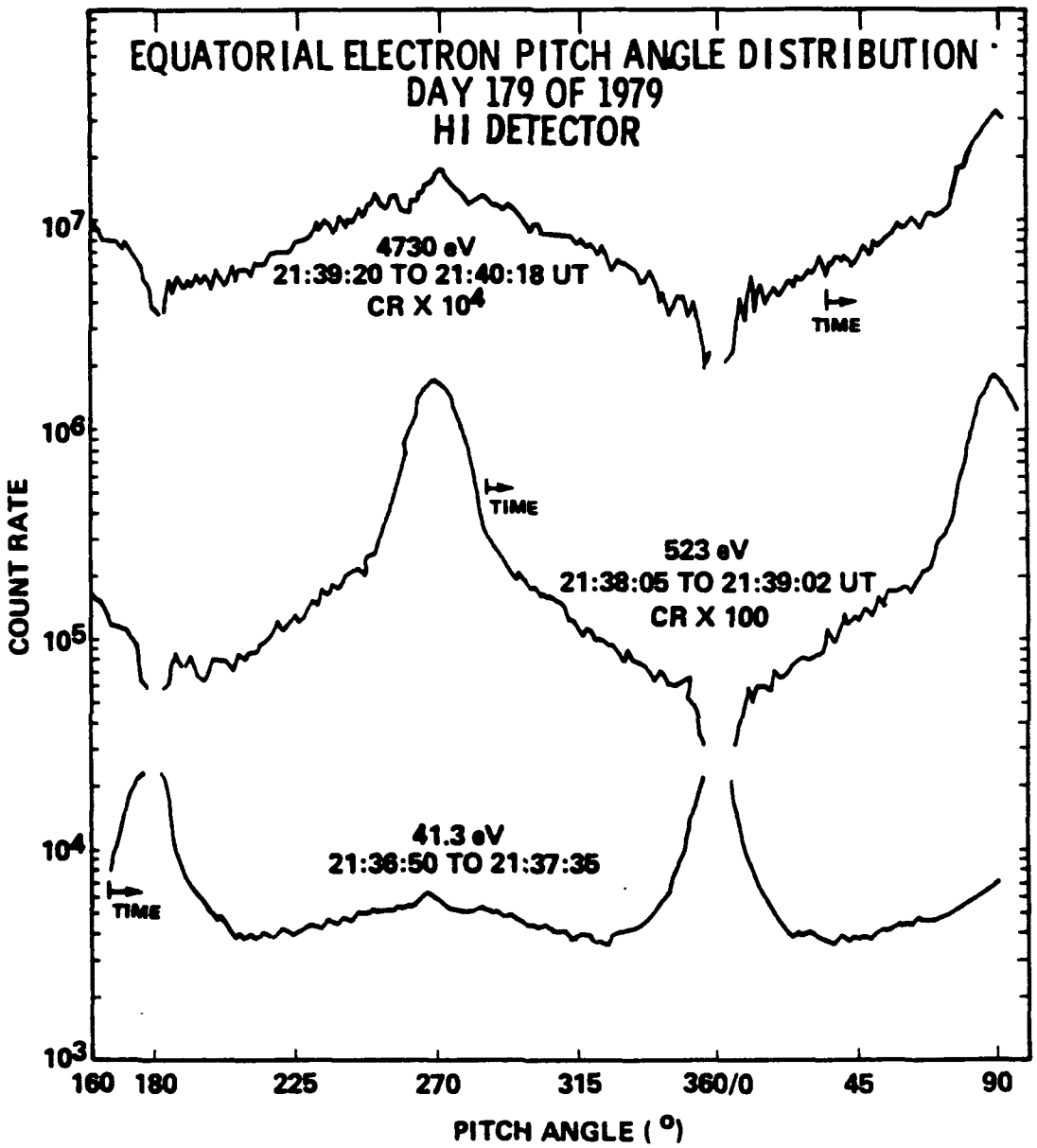

Figure 5. Electon Pitch Angle Distribution, SCATHA Day 179 of 1979. [Ref. 5]

the equatorial ion and electron pitch angle distributions as observed by the SCATHA spacecraft on day 179 of 1979. These data are taken at 1000 local time, $L = 5.5$, at the magnetic equator. The count rate is plotted as a function of the pitch angle through 360 degrees, with pitch angles greater than 180 degrees corresponding to looking earthward. The count rate is peaked at pitch angles of 90^0 and 270^0 indicating equatorially trapped distributions. The 41 eV electron distribution in Figure 5 shows peaks at 0^0 and 180^0, in addition to peaks at $90^0/270^0$. This indicates that there is also a field aligned component to the electron distribution. The equatorial ion and electron energy distributions are shown in Figure 6. The $\log_{10} f$ is plotted as a function of energy for pitch angles near 90^0. The inset in this figure shows the low energy portion of the distribution for ions. The flattening out of this portion indicates a non-thermal character of the plasma. This data has been previously examined by Olsen [Ref. 5] and will be examined in greater detail in Section III.

The data from day 41 of 1979 provide a second example of an equatorially trapped plasma seen by the SCATHA spacecraft. These data were taken at 2100 local time, and $L = 5.3$. Figures 7 and 8 are plots of the $\log_{10} f$ versus pitch angle for ions and electrons respectively. Both Figures 7 and 8 show peaks at 90^0 pitch angle, again indicating that the particles are equatorially trapped. A mass analysis of these data with the Light Ion Mass Spectrometer shows that the ions are primarily H^+. The lowest energy ions (7.25 eV) show evidence of a field-aligned distribution, as well (Fig. 7). All of these data show a characteristic decrease in the width of the trapped distribution with increasing energy. This characteristic of the data shown in Figures 4,5,7,and 8 suggests that the data may be fitted with a bi-Maxwellian distribution function. This will be pursued below.

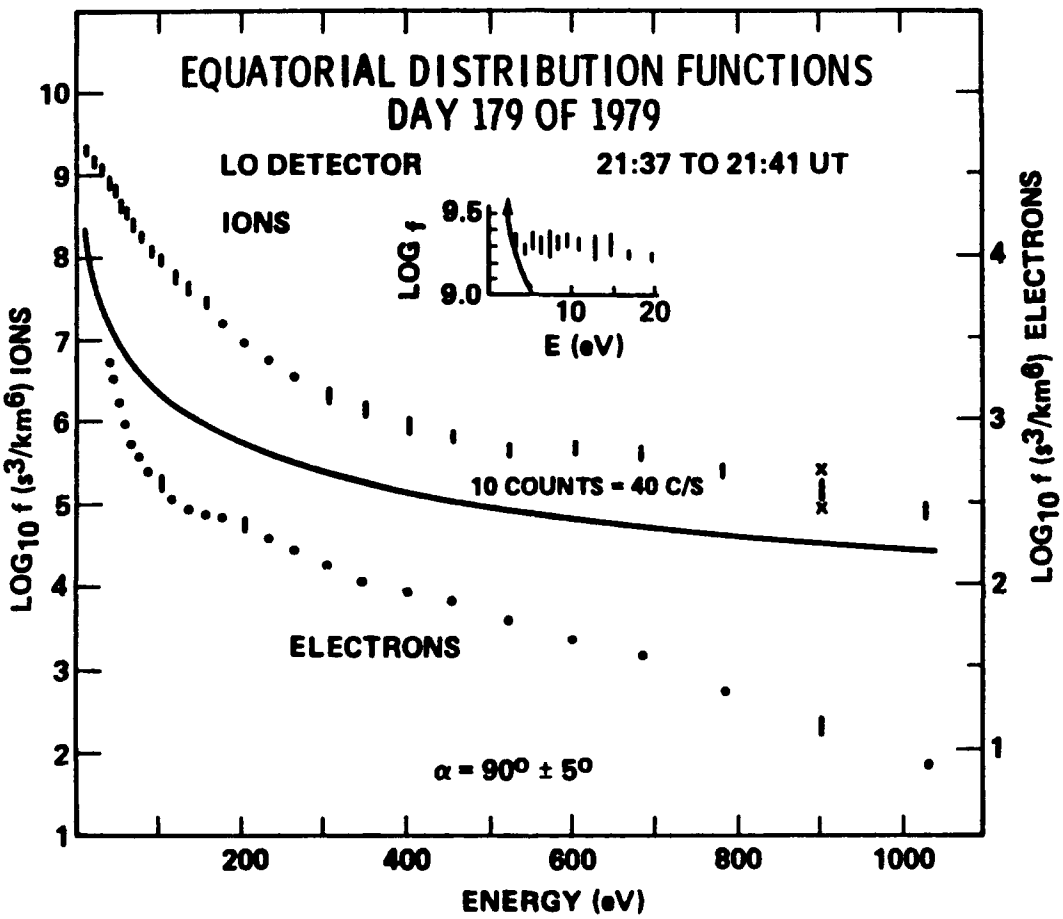

Figure 6. Ion and Electron Energy Distribution, SCATHA Day 179 of 1979. [Ref. 4]

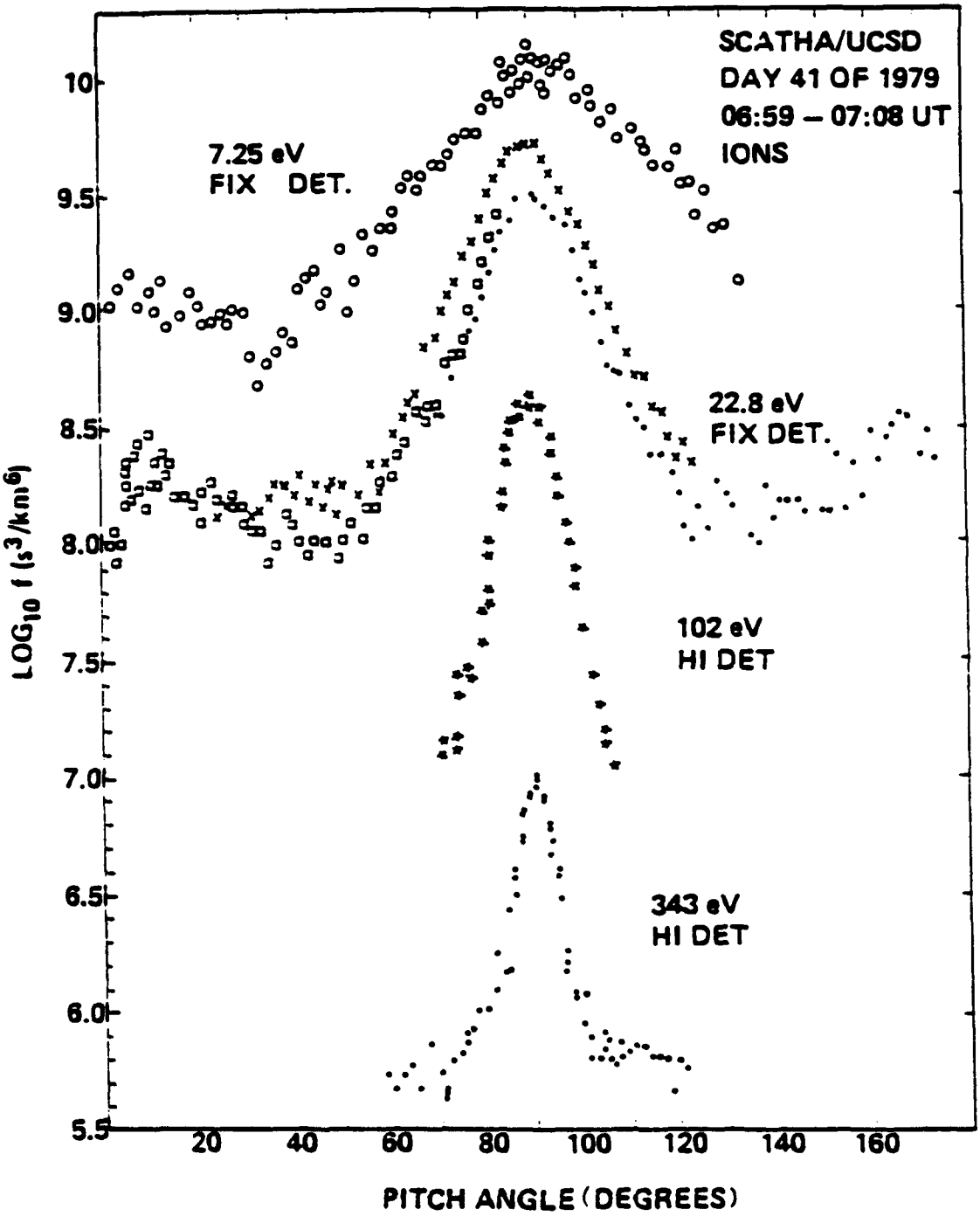

Figure 7. Ion Pitch Angle Distribution, SCATHA Day 41 of 1979.

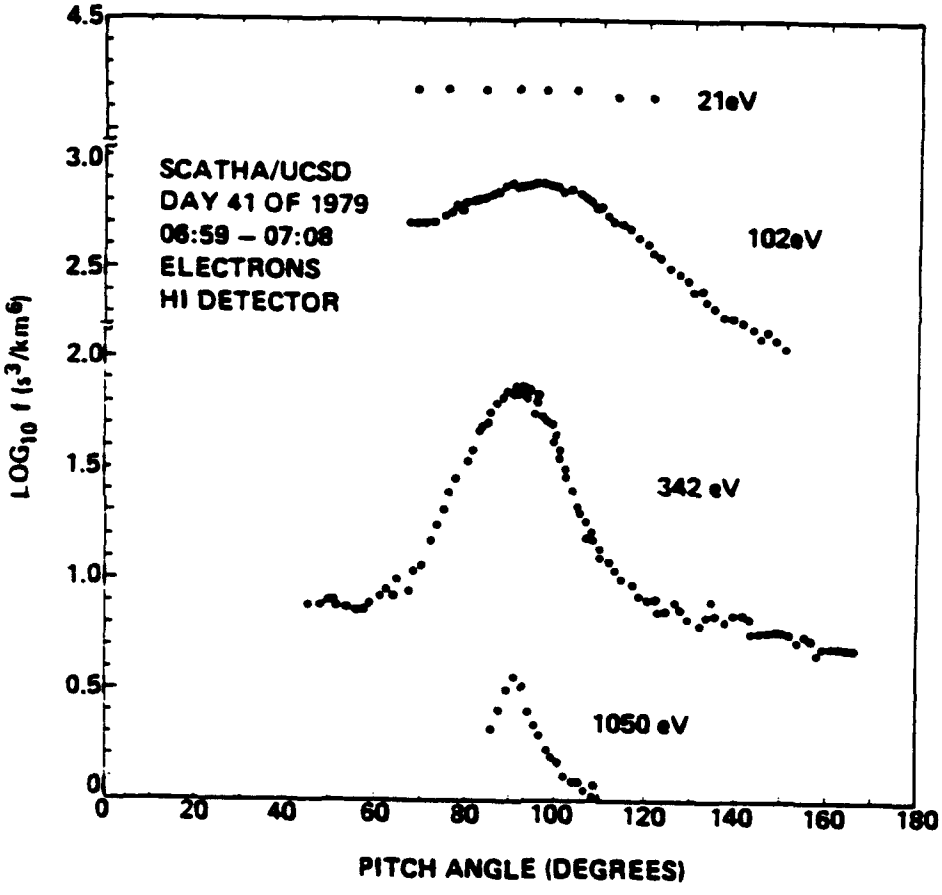

Figure 8. Electon Pitch Angle Distribution, SCATHA Day 41 of 1979.

2. Dynamics Explorer-1 (DE-1)

The Dynamics Explorer-1 (DE-1) spacecraft was launched on August 3, 1981 in an elliptical polar orbit with an apogee of 4.9 R_E and perigee of 1.1 R_E geocentric. The general shape of the spacecraft is a 1 meter long polygon with a diameter of approximately 1.4 m. The spin rate is 6 seconds, with an axis perpendicular to the orbit plane. The data analyzed here were taken using the Retarding Ion Mass Spectrometer (RIMS) instrument. Figure 9 shows the DE-1 spacecraft and the location of the RIMS detector on it. [Ref. 6.7]

The RIMS instrument consists of three sensor heads. One head (radial sensor) is mounted to look radially out of the spacecraft perpendicular to the spin axis while the other 2 (±Z) sensor heads look along the spin axis. Each of the sensor heads consists of a Retarding Potential Analyzer (RPA) followed by an Ion Mass Spectrometer (IMS). The RPA voltage sweeps from 0 to 50 Volts, providing energy analysis, while the IMS provides for mass analysis in the 1 to 32 amu range. Pitch angle distributions are obtained from the radial sensor for ions in the 0 to 50 eV range. This sensor has a radial aperture of $\pm 10^0$ in the plane perpendicular to the spin axis and $\pm 55^0$ perpendicular to the spin plane. The spin axis detectors have a resolution of $\pm 55^0$, and are looking in the direction perpendicular to the magnetic field. [Ref 6,7]

Lower altitude (e.g., below SCATHA) observations of equatorially trapped ions have been made by the RIMS detector on DE-1. The data from day 126 of 1982 provides one example of an equatorially trapped plasma. The satellite is near 4.6 R_E with an equator crossing at 1100 UT. Figure 10 is a spin-time spectrogram for H^+ and He^+, from 0930 to 1230 UT. The data was taken by the radial detector with a 0 Volt retarding potential. The spin-phase is

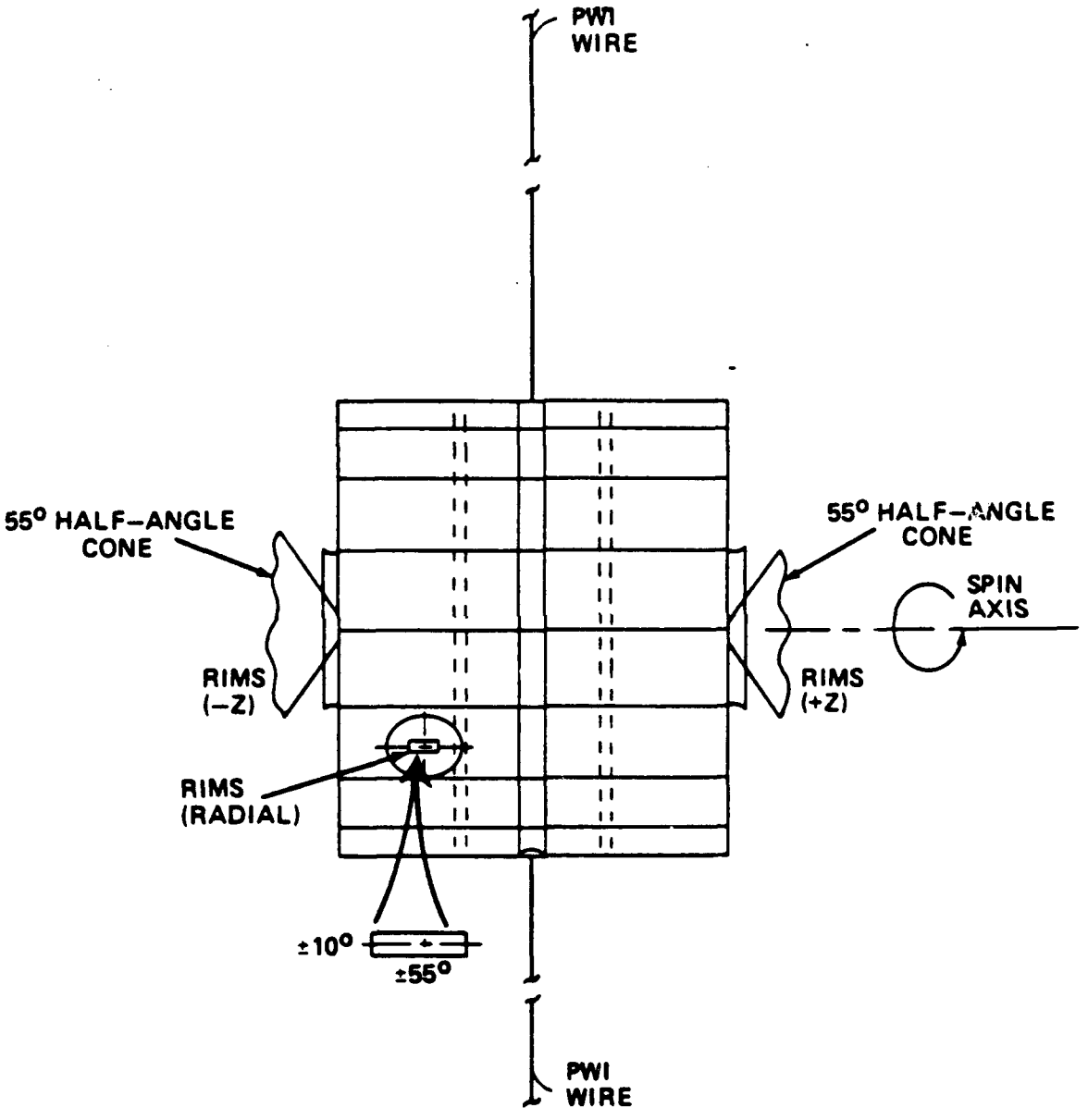

Figure 9. RIMS Detector on the Dynamics Explorer-1 spacecraft. [Ref. 7]

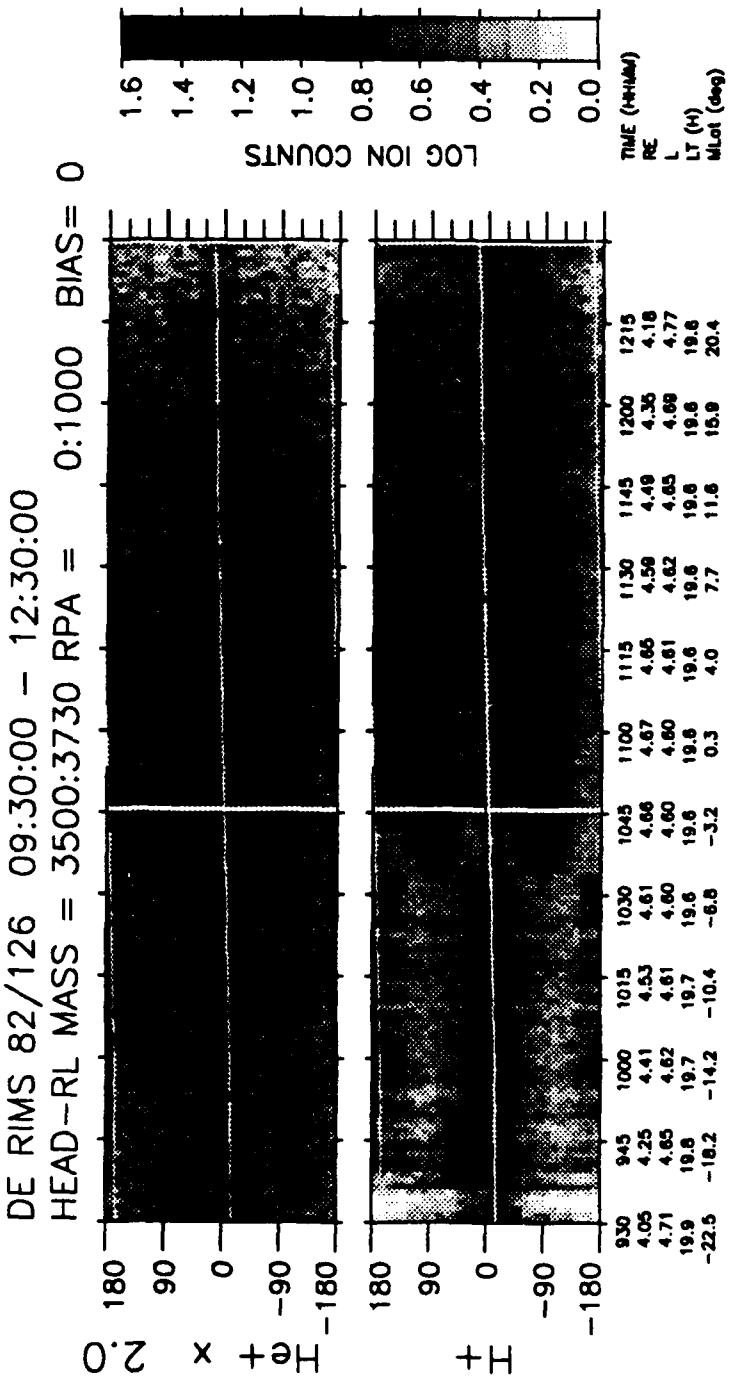

Figure 10. DE-1 Spin-time Spectrogram, Day 126 of 1982.

shown on the left from -180^0 to 180^0 with 0^0 being in the satellite velocity (RAM) direction. The pitch angle of the sensor is shown by the white lines running along the spectrogram. The center line shows the spin phase for 0^0 pitch angle, and the top and bottom line show spin phase for 180^0 pitch angle. The $\log_{10}$ (ion counts) is scaled according to the "color" bar to the right of the spectrogram with white being minimum and black a maximum. From this spectrogram we can see that for H^+, there is a field aligned distribution (α peaked at 0^0,180^0) which becomes an equatorially trapped distribution (α peaked at 90^0,270^0) at 1035 UT [Ref 8]. The He^+ data are similar with count rate being 1 to 2 orders of magnitude lower than those for H^+. Figure 11 is a line plot of the $\log_{10}$(count rate) versus pitch angle for ions with peaks at 90^0 and 270^0. These data were taken at 1055 local time, and $L = 4.6$. The data for this day has been previously examined by Olsen [Ref. 5].

The second example of equatorially trapped ions at $L = 4.6$ comes from the data taken on day 315 of 1983. The satellite crosses the equator at approximately 0545 LT and L=4.6. Figure 12 is a spin-time spectrogram from 0430 to 0700 LT. High count rates are seen for $\alpha \approx 90^0$ near the equator. Figure 13 is an RPA-time spectrogram for H^+ and He^+ taken by the +Z ($\alpha \approx 90^0$) sensor, for the RPA voltage from 0 to 50 V. These spectrograms show low energies and counts away from the equator and high fluxes and energies near the equator. These figures are both indicative of equatorially trapped plasmas. Figure 14 is a line plot of the $\log_{10}$(count rate) versus pitch angle for ions with peaks at 90^0 and 270^0. This data was taken at 0555 local time. Figures 11 and 14 indicate equatorially trapped plasmas, and their shapes also suggest that the data may be fitted with a bi-Maxwellian. The data for both days 126 and 315 will be examined in further detail in Section III.

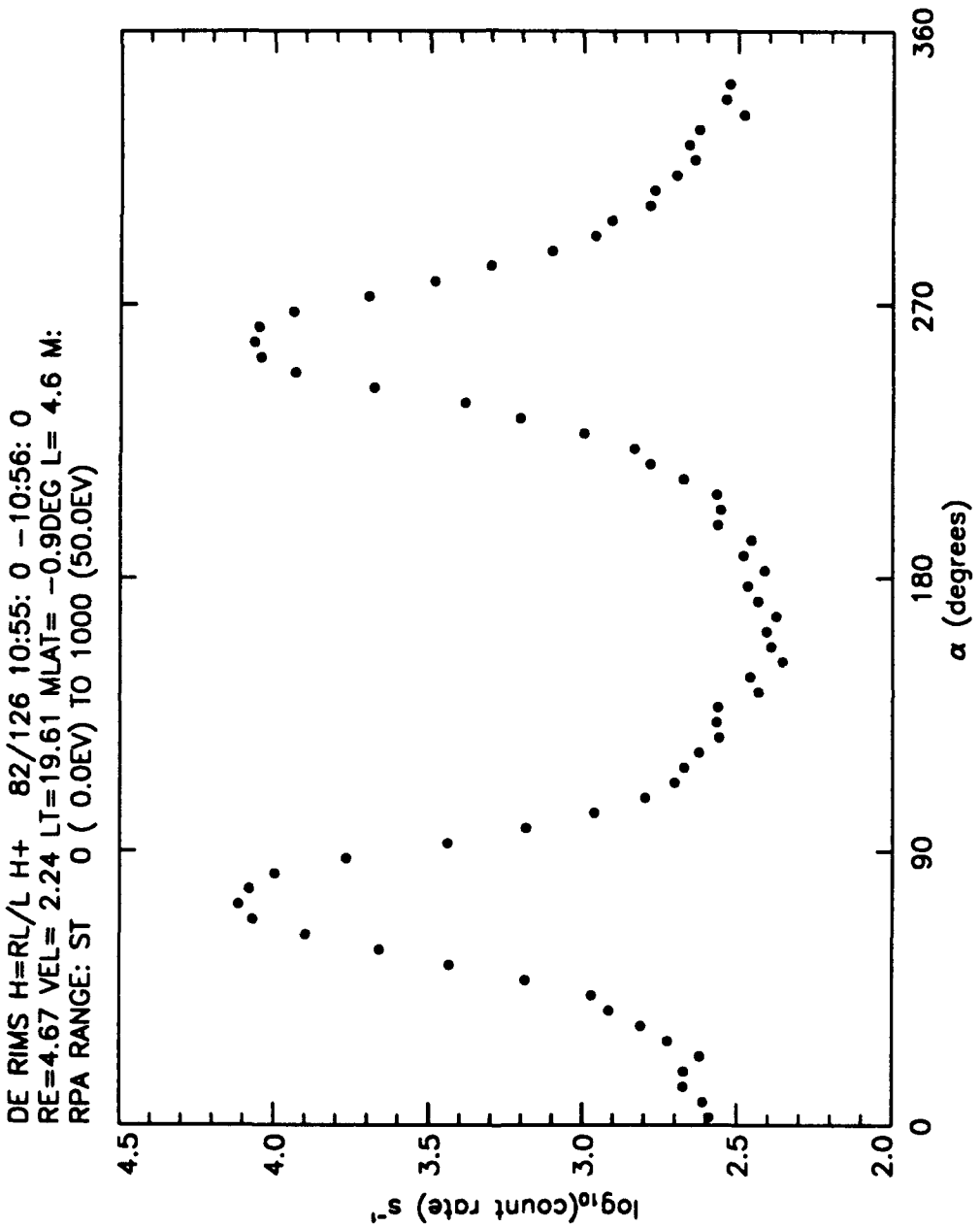

Figure 11. Ion Pitch Angle Distribution, DE-1 Day 126 of 1982. [Ref. 8]

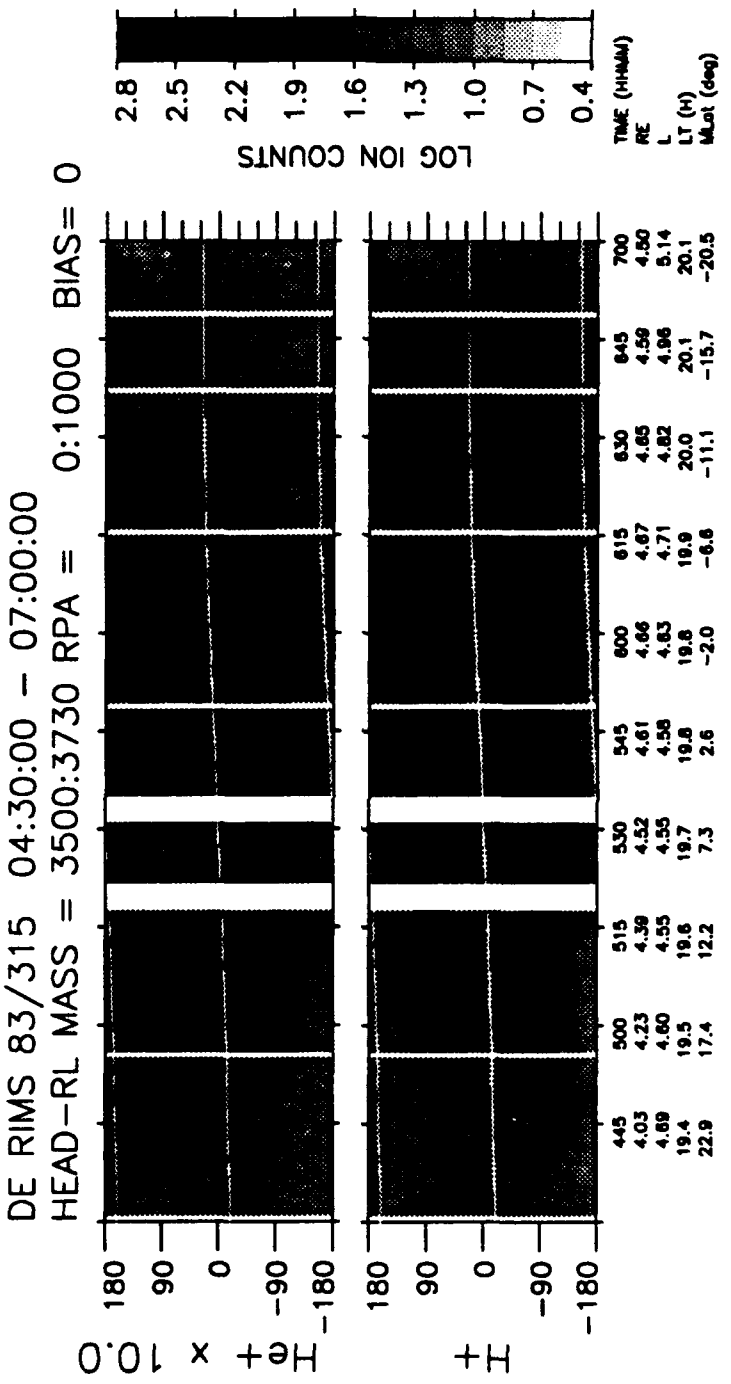

Figure 12. DE-1 Spin-time Spectrogram, Day 315 of 1982.

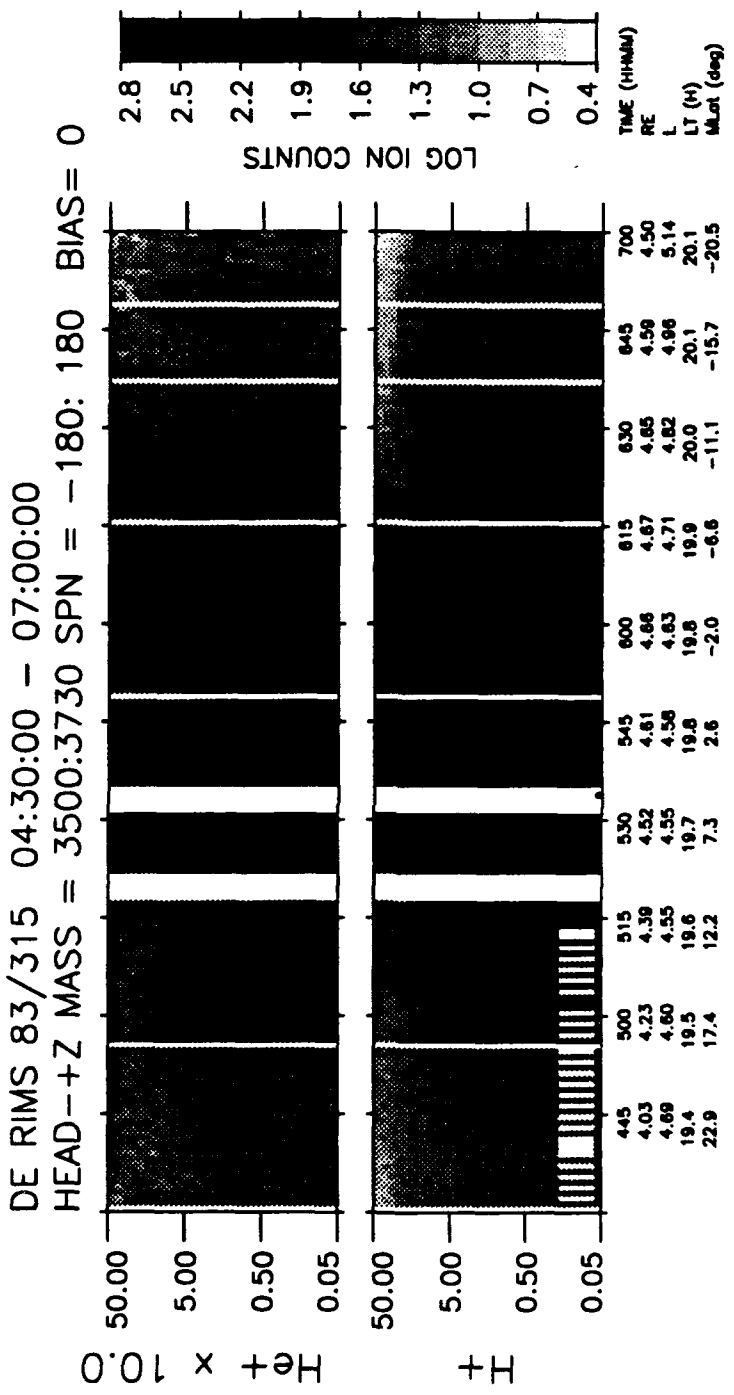

Figure 13. DE-1 RPA-time Spectrogram, Day 315 of 1982.

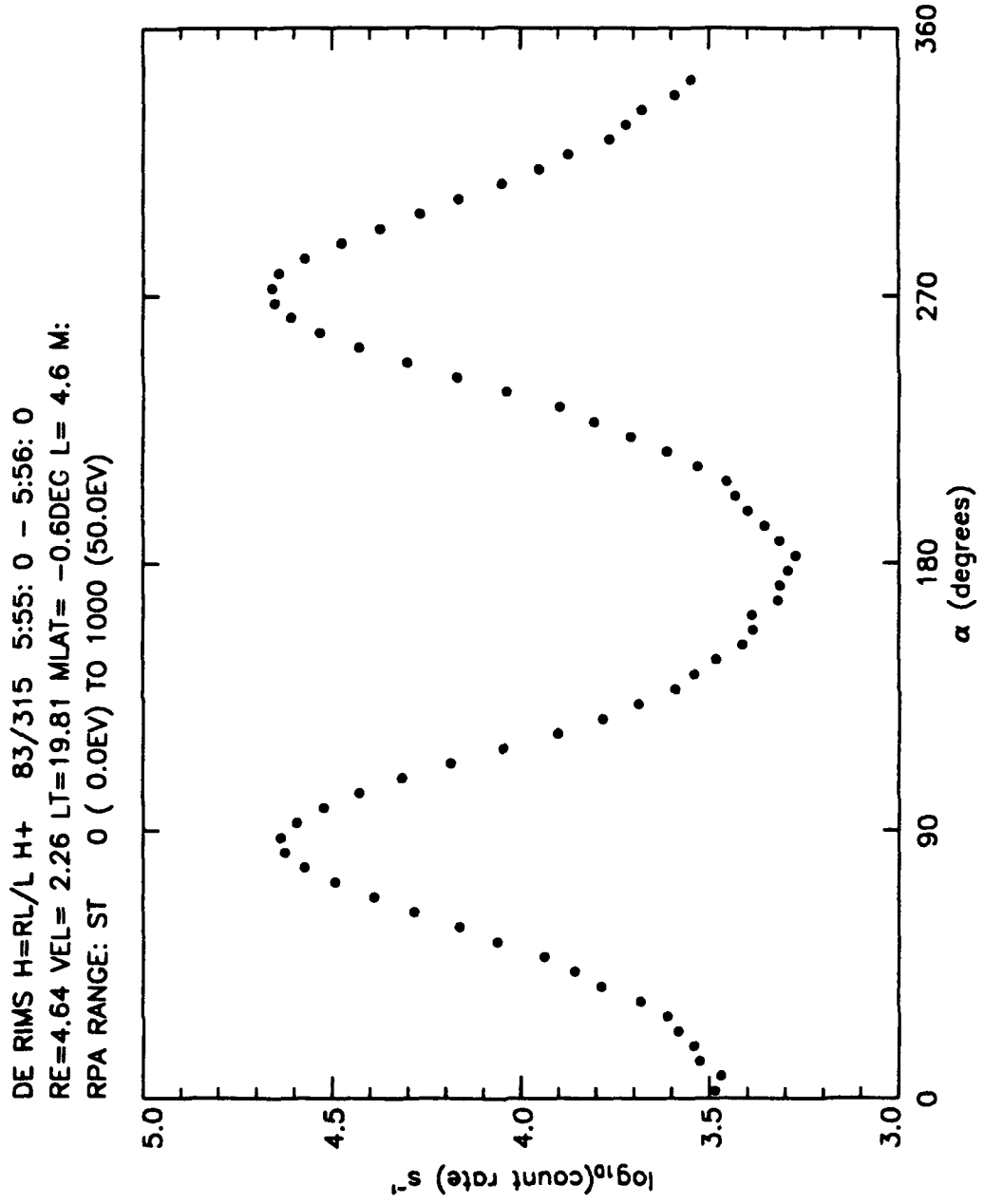

Figure 14. Ion Pitch Angle Distribution, DE-1 Day 315 of 1983. [Ref. 8]

Olsen [Ref. 9] has shown that there is often a relative density minimum observed at the magnetic equator, by means of total electron density measurements. Figure 15 shows such a density profile as observed by the DE-1 spacecraft on day 296 of 1983. The bottom portion of the figure is a plot of density versus magnetic latitude as determined from the plasma wave data. In the top portion of the figure the density has been normalized by the factor $(L/4.5)^4$ to eliminate the variations in density induced by the radial component of the satellite orbit. This density profile is typical when a density minimum is observed. The trapped ions typically observed with RIMS are confined to $\pm 10^0$ magnetic latitude during this orbit, and are typically found whenever such mimina are observed.

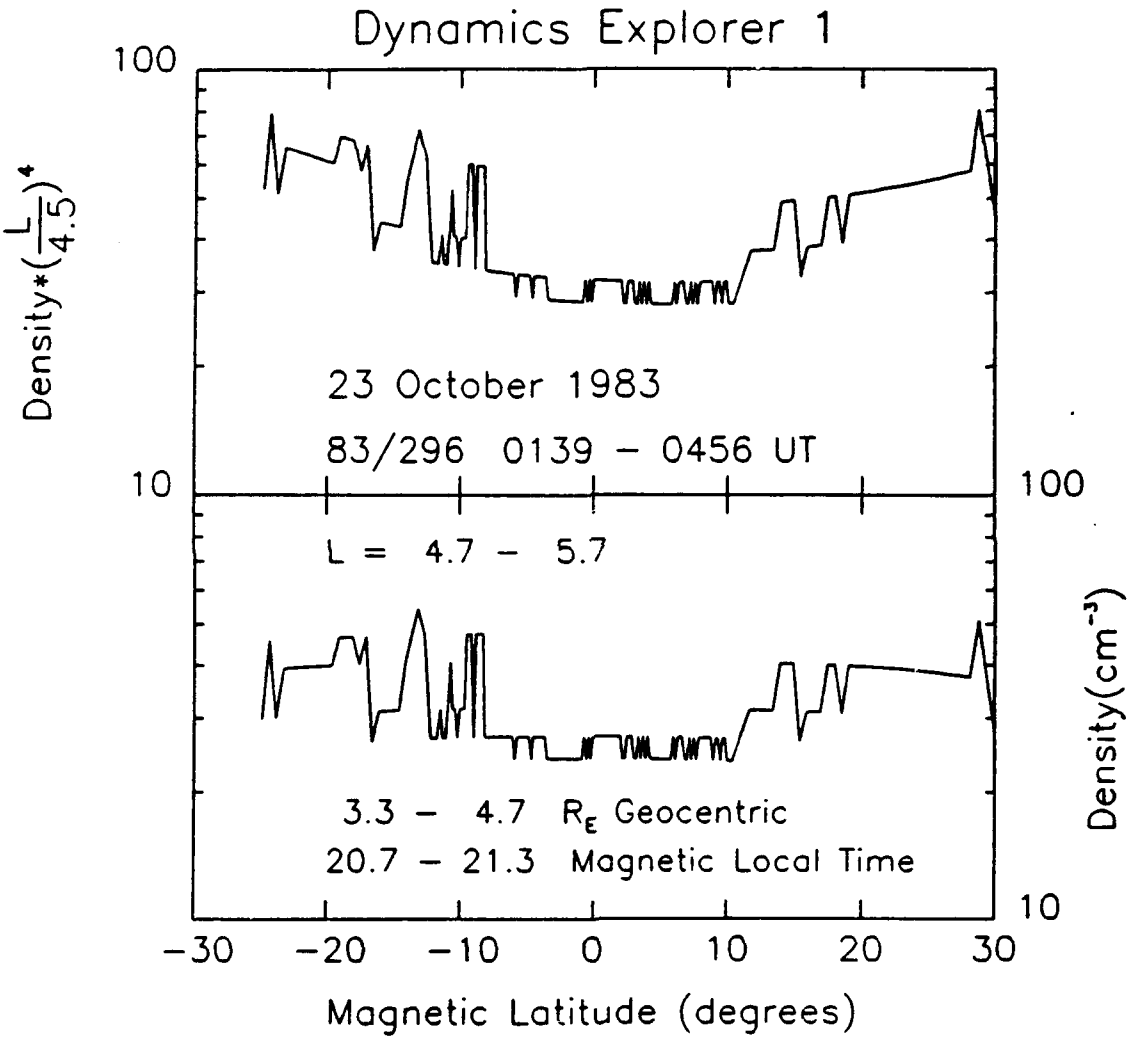

Figure 15. Density Minimum Profile, DE-1 Day 296 of 1983. [Ref. 9]

III. BI-MAXWELLIAN DISTRIBUTIONS

The purpose of examining data from the P78-2 (SCATHA) and the Dynamics Explorer-1 (DE-1) spacecraft is to show that observed distributions of equatorially trapped plasmas may be described as a bi-Maxwellian. In fitting the observations with a bi-Maxwellian, the characteristic temperatures (T_{perp} and T_{par}) and the density of the plasma may be determined. This section will present three examples of equatorially trapped plasmas which may be fitted with a bi-Maxwellian distribution.

A. SCATHA, DAY 179 OF 1979

Figures 16 and 17 show the ion and electron energy distributions, previously shown in Figure 6, up to 500 eV. These data were measured by the LO detector at the magnetic equator with a pitch angle near 90^0. A fit to the ion data in the 2 to 100 eV range gives a temperature (T_{perp}) of 25 eV and a density ($4\pi\partial n/\partial\Omega$) of 7.2 cm^{-3}. The fit in the 100 to 350 eV range gives a temperature of 55 eV and density of 2.8 cm^{-3}. The fit to the electron data in the 2 to 100 eV range gives a temperature of 27 eV and density of 1.7 cm^{-3}. The fit to the 100 to 1000 eV data gives a temperature of 251 eV and a density of 2.4 cm^{-3}. Here, the fitting process assumes the distributions are isotropic. Hence, the density determined in these fits does not give the true density. The "density" obtained in these fits is therefore designated ($4\pi\partial n/\partial\Omega$). These results are consistent with those reported by Olsen. [Ref. 5]

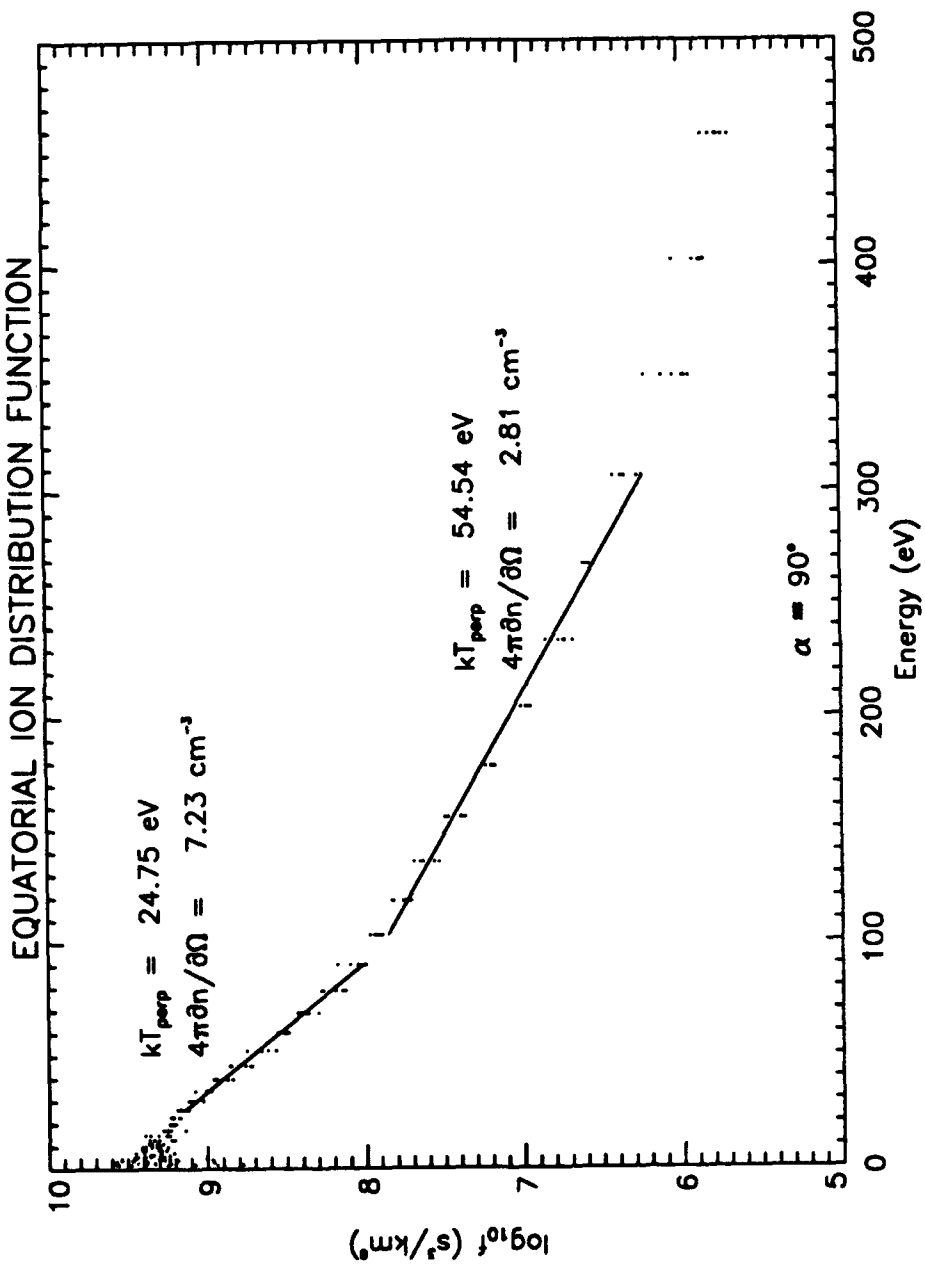

Figure 16. Ion Energy Distribution Function, SCATHA Day 179 of 1979.

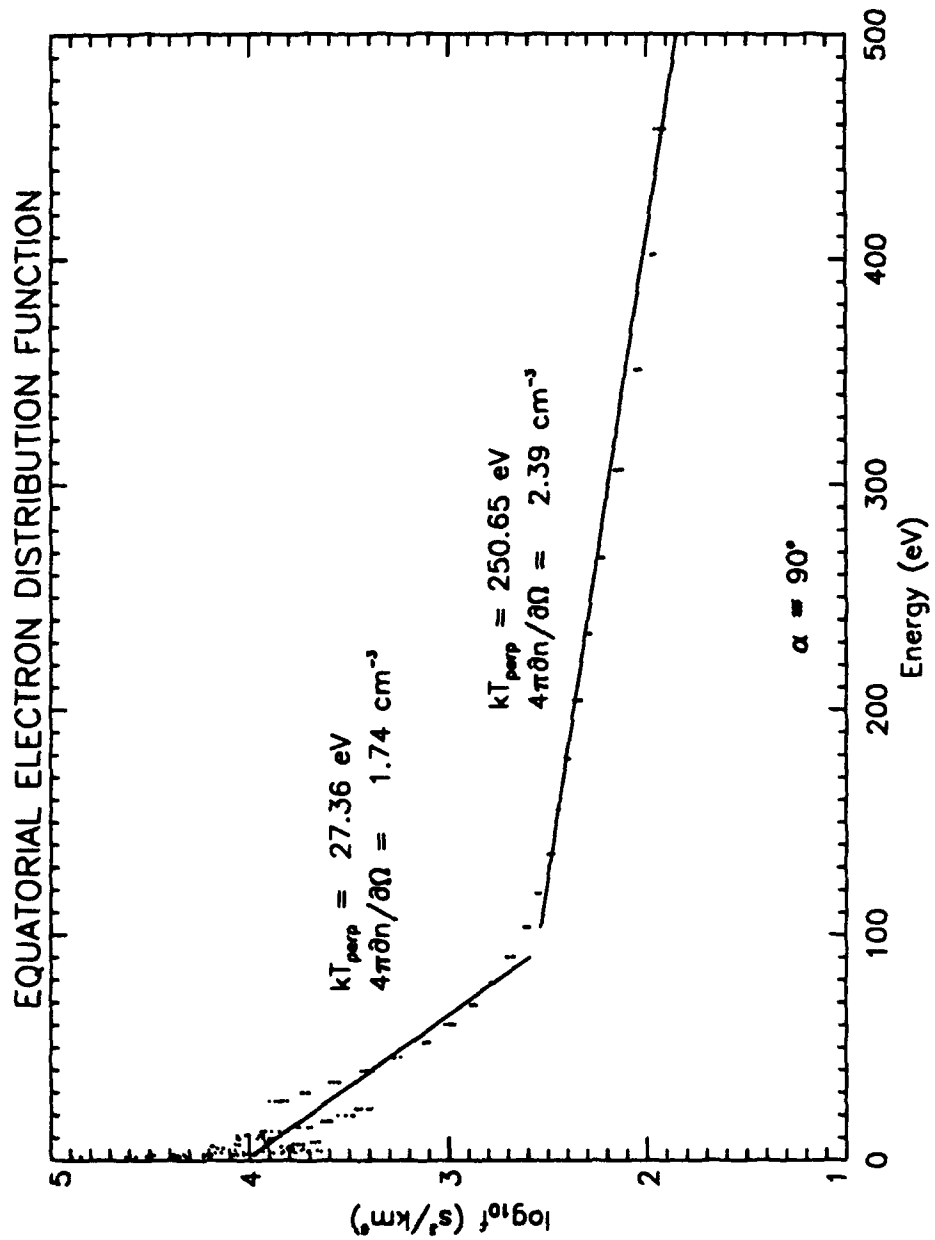

Figure 17. Electron Energy Distribution Function, SCATHA Day 179 of 1979.

The pitch angle distributions can be used to obtain the parallel temperature, and hence a more accurate density. The ion pitch angle distributions, shown in Figure 4, were examined for the 11.2, 41 and 103 eV energies. The electron pitch angle distributions, shown in Figure 5, were examined at 41.3 and 523 eV. The pitch angle distributions, as measured by the HI and FIX detectors, for ions and electrons are shown in Figures 18 and 19. The $\log_{10} f$ is linearly related to $\cos^2\alpha$ with a slope proportional to the ratio of the perpendicular to the parallel temperature. This relationship is given by

$$\log_{10} f = \log_{10}\left[n\left(\frac{m}{2\pi k T_{perp}}\right)\left(\frac{m}{2\pi k T_{par}}\right)^{1/2}\right] - \frac{E\log_{10}(e)}{kT_{perp}} + \frac{E\log_{10}(e)}{kT_{perp}}\left(1 - \frac{kT_{perp}}{kT_{par}}\right)\cos^2\alpha.$$

If the plasma can be described as a bi-Maxwellian, the data will fall along a straight line, when the angular distribution is plotted vs $\cos^2\alpha$. The initial portion of each pitch angle distribution follow a reasonably straight line in Figures 18 and 19. The angular distributions show a deviation from linearity for $\cos^2\alpha$ greater than approximately .05, particularly in the ion data. This is due to the presence of a warm isotropic background.

The solid lines in Figures 18 and 19 are the results of a bi-Maxwellian fit using the perpendicular temperature and the density obtained from the fits to the energy distributions in Figures 16 and 17. The only free parameter left then is the parallel temperature. In addition a warm isotropic background is included with the isotropic density being five percent of the total density. The parallel temperatures of the ions and electrons were estimated from the fits to the data, as summarized in Table 1. In Figure 18, for the 11.2 eV ions the amplitude of the fit appears to be too high. This stems from the fact that the distribution function flattens below 20 eV, as shown in Figure 6. This is a symptom of quasi-linear diffusion. The fitted density obtained from the energy distributions

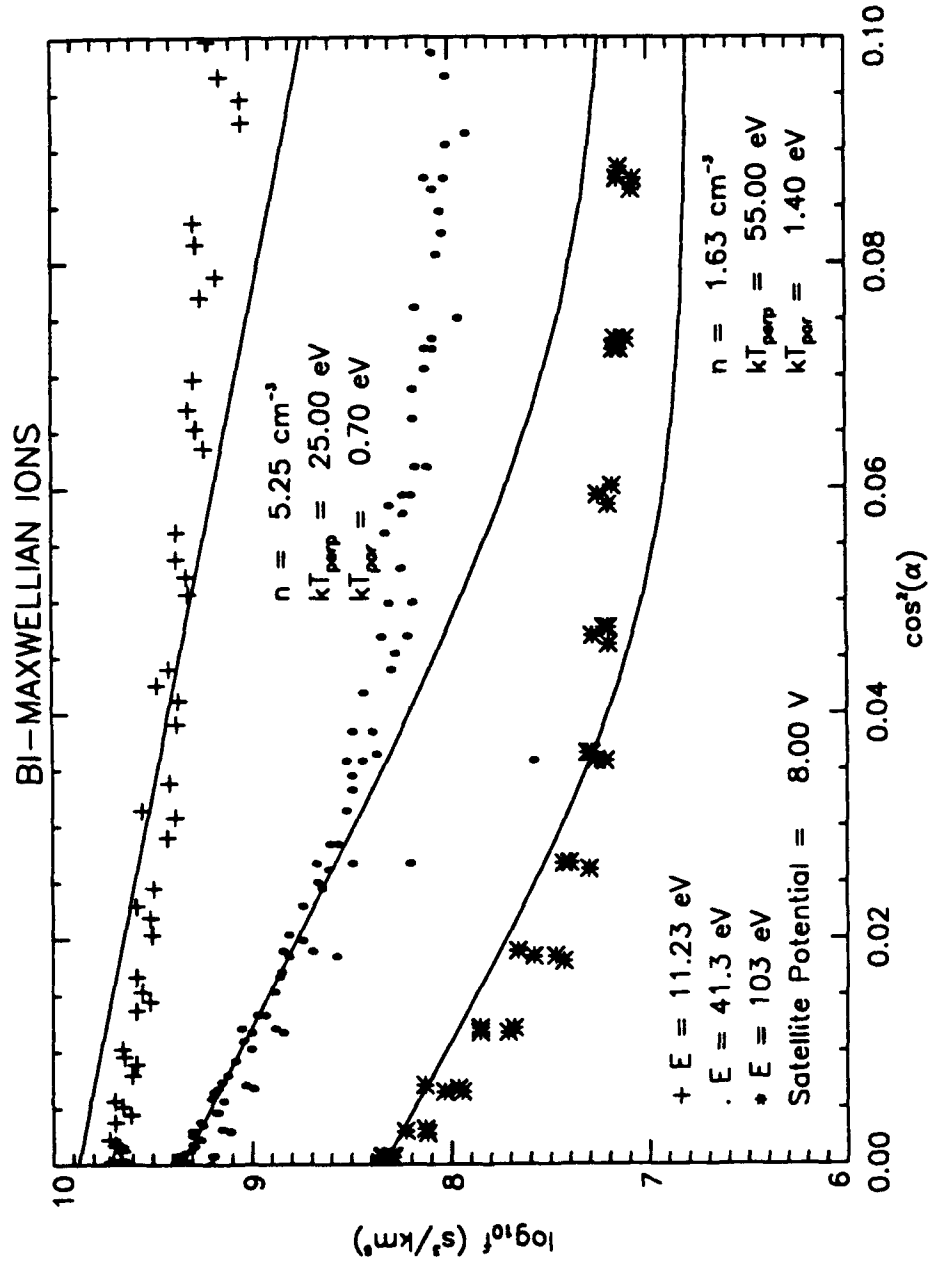

Figure 18. Ion Pitch Angle Distribution.

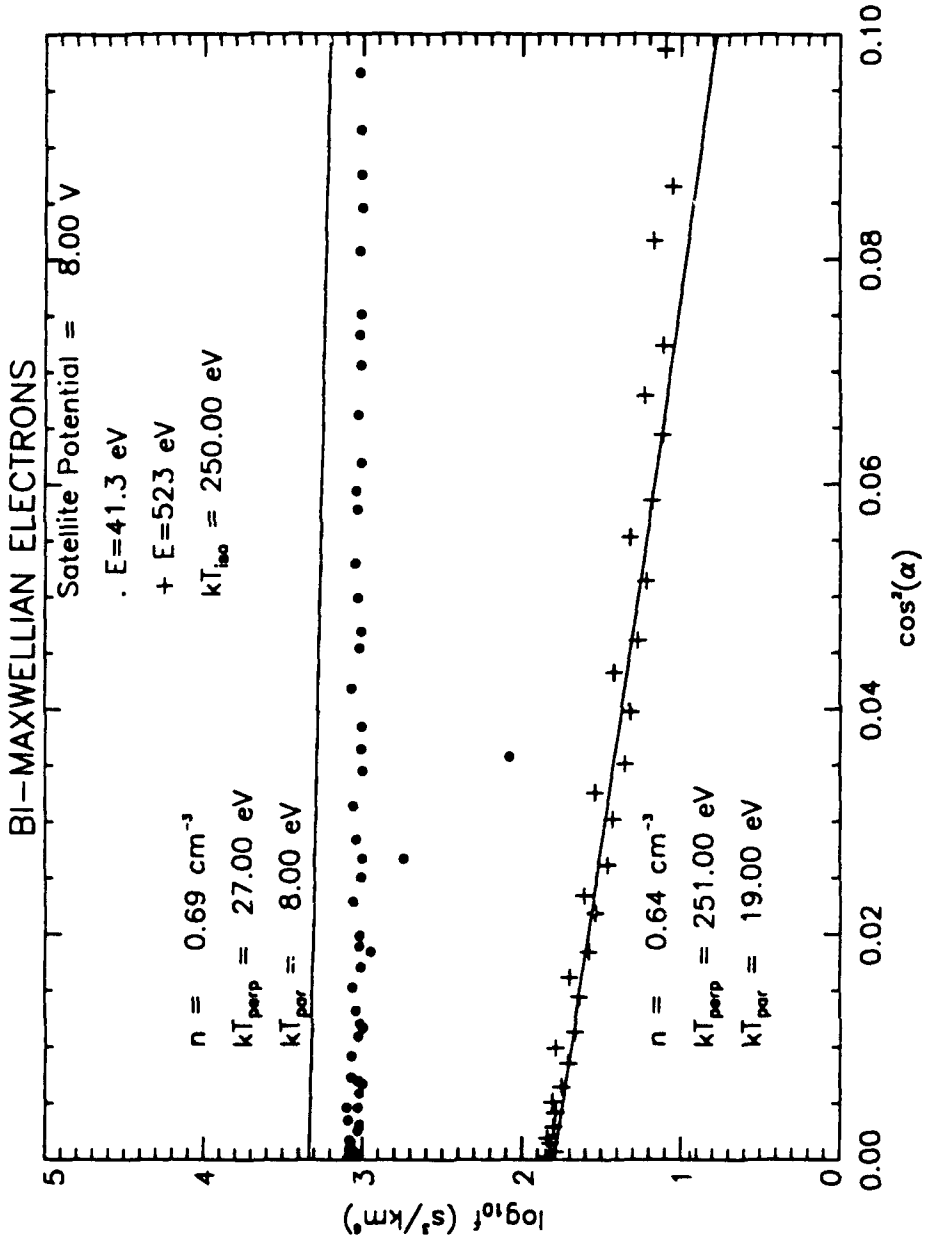

Figure 19. Electron Pitch Angle Distribution.

(Figures 16,17) must be corrected to account for the anisotropy and the spacecraft potential by the factor

$$n = \left[\frac{4\pi\partial n}{\partial\Omega}\right] \frac{e^{\frac{q\phi}{kT_{perp}}}}{\sqrt{T_{perp}/T_{par}}}.$$

The data suggest that the spacecraft potential is approximately +8V. The temperatures and the corrected density are summarized in Table 1.

TABLE 1. DENSITY AND TEMPERATURES, SCATHA

Day 179 of 1979				
	Ions (11.2 & 41 eV)	Ions (103 eV)	Electrons (41.3 eV)	Electrons (523 eV)
Density (cm^{-3})	5.3	1.6	0.7	0.6
kT_{perp} (eV)	25	55	27	251
kT_{par} (eV)	0.7	1.4	8	19

B. DE-1, DAY 126 OF 1982

Figure 20 is a plot of $\log_{10}$ (count rate) versus $\cos^2\alpha$ for the data taken from 10:55 to 10:56 at a magnetic latitude of -0.9^0. Figure 21 is a similar plot for data taken from 10:40 to 10:41, at a magnetic latitude of -4.4^0. The solid lines in these figures are the angular distribution which RIMS would show for an equatorial bi-Maxwellian with kT_{perp} = 11 eV, kT_{par} = 0.4eV, and a density of

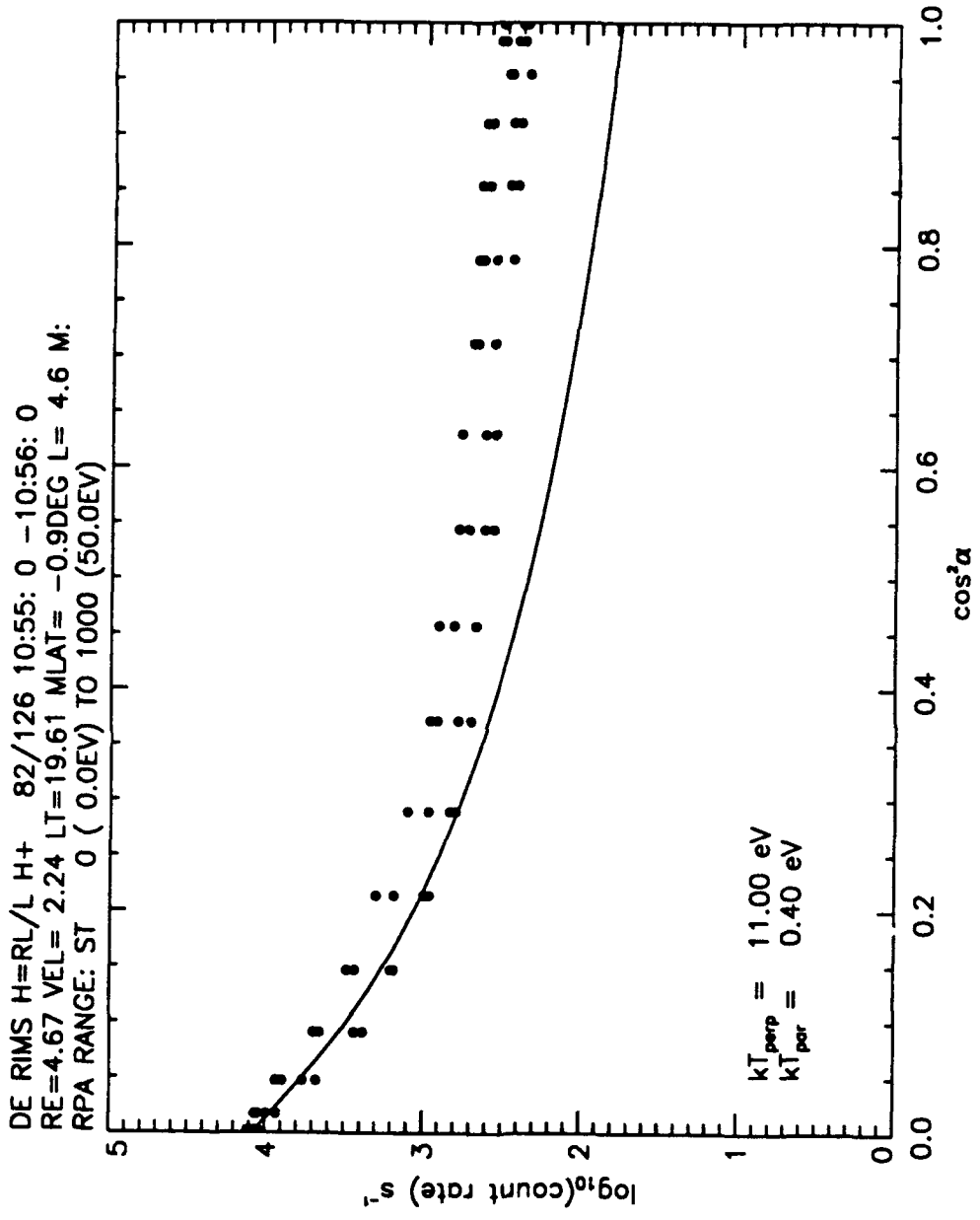

Figure 20. DE-1 Pitch Angle Distribution, Day 126 of 1982, 10:55 to 10:56

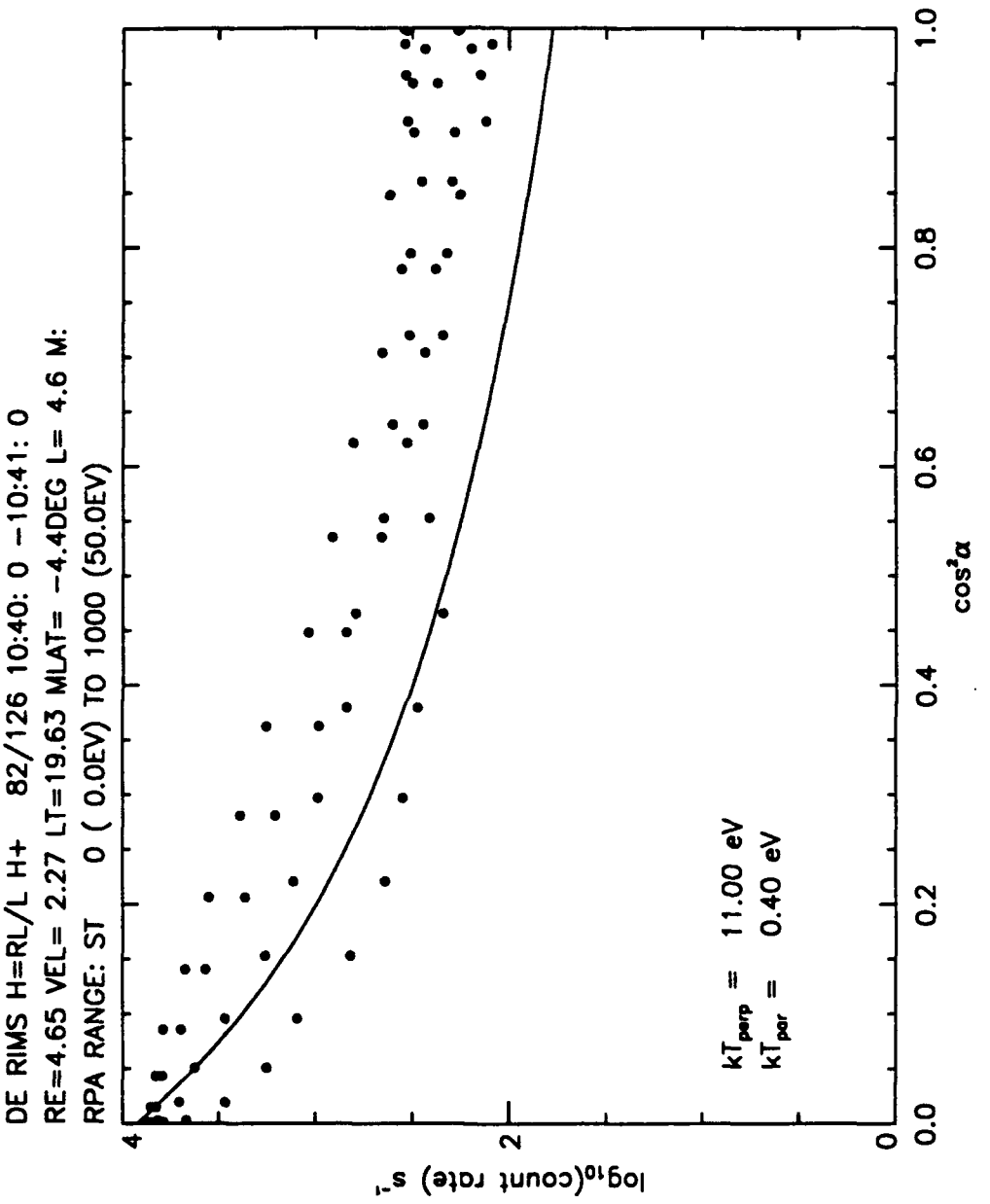

Figure 21. DE-1 Pitch Angle Distribution, Day 126 of 1982, 10:40 to 10:41

approximately 5 cm^{-3}. The equatorial distribution has been mapped to the latitude where the particle measurements were taken, assuming there is no parallel electric field.

C. DE-1, DAY 315 OF 1983

Figures 22 and 23 show the data from 5:55 to 5:56 at $\lambda = -0.6^0$ and from 5:25 to 5:26 for $\lambda = 8.9^0$. An equatorial bi-Maxwellian can be fitted to these data giving temperatures of kT_{perp}= 20 eV, kT_{par}= 2.5 eV. The density is poorly defined, due to questions about the detector efficiency, but is approximately 10-30 cm^{-3}.

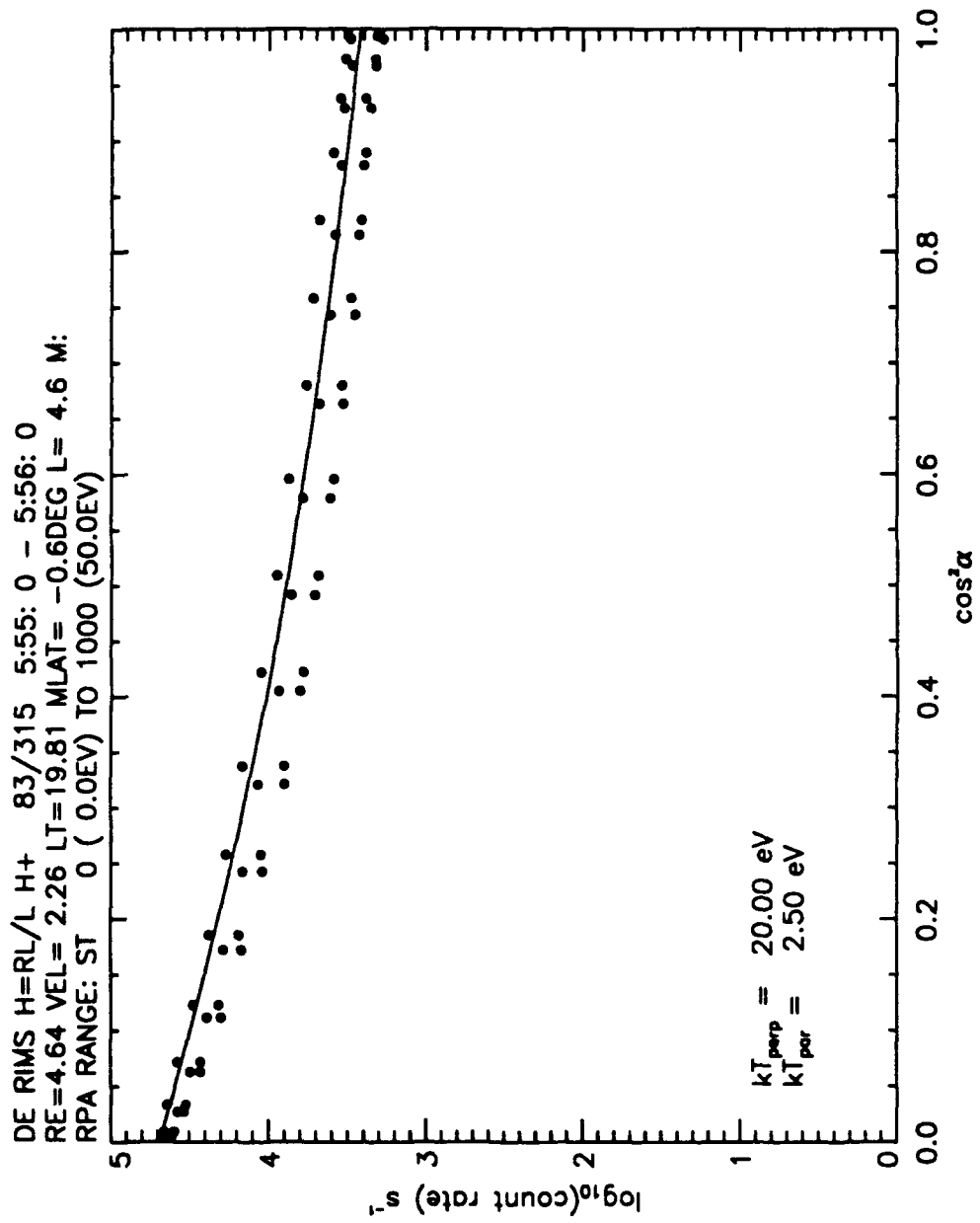

Figure 22. DE-1 Pitch Angle Distribution, Day 315 of 1982, 5:55 to 5:56

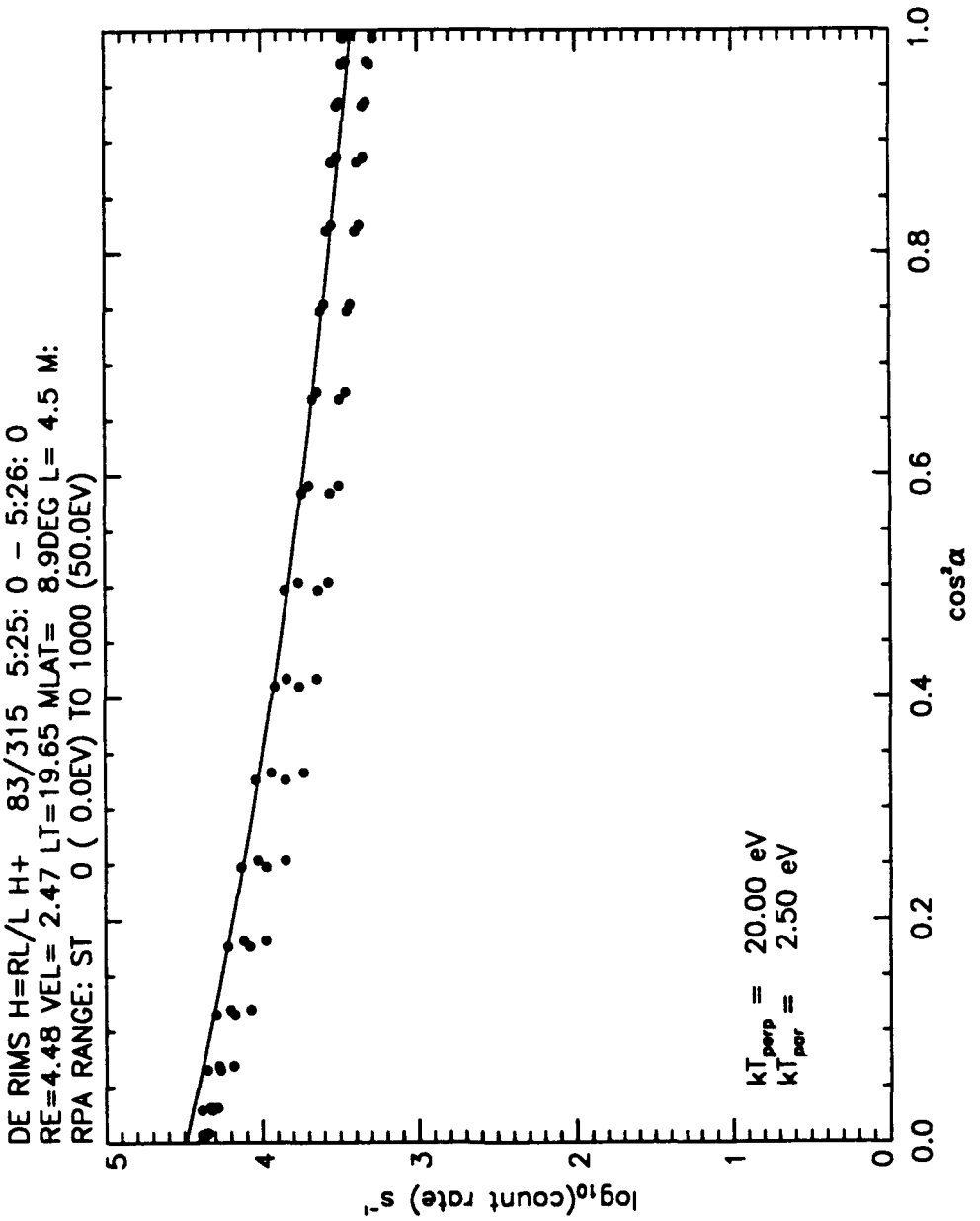

Figure 23. DE-1 Pitch Angle Distribution, Day 315 of 1982, 5:25 to 5:26

IV. MODEL

A. BI-MAXWELLIAN

It has been seen from the data taken by the UCSD/SC-9 and RIMS instruments on the SCATHA and DE-1 satellites that there is a thermal plasma population trapped within a few degrees of latitude of the magnetic equator. These populations may be characterized as bi-Maxwellian distributions. We want to examine how bi-Maxwellian distributions evolve with magnetic latitude and the consequences for parallel electric fields. Figure 24 is a contour plot of a bi-Maxwellian distribution in velocity space at the magnetic equator. The color bar to the right of the figure shows the scale for the distribution function. Figure 25 is a contour plot of the same distribution that has been mapped to 10^0 latitude. It can be seen from the comparison of these figures that the distribution function decreases in the perpendicular velocity direction as the latitude increases. This is due to to the increase in the perpendicular component of the velocity as the particles travel from a relatively weak to a stronger magnetic field region. The equatorial density for both Figures 24 and 25 is 10 cm^{-3}, dropping to 4.6 cm^{-3} at 10^0 latitude. If a constant electric field is now added, pointing away from the equator, the initial equatorial distribution will not be changed. Figure 26 shows how the distribution maps to $\lambda = 10^0$ for a 0.1 $\mu V/m$ electric field. As the distribution function is mapped off of the equator, the electric field accelerates the low energy ions away from the equator. This can be seen in Figure 26 where the distribution function has been mapped to 10^0 latitude. The black portion in the middle is the low energy portion of the distribution function that has been excluded. Outside this region the distribution

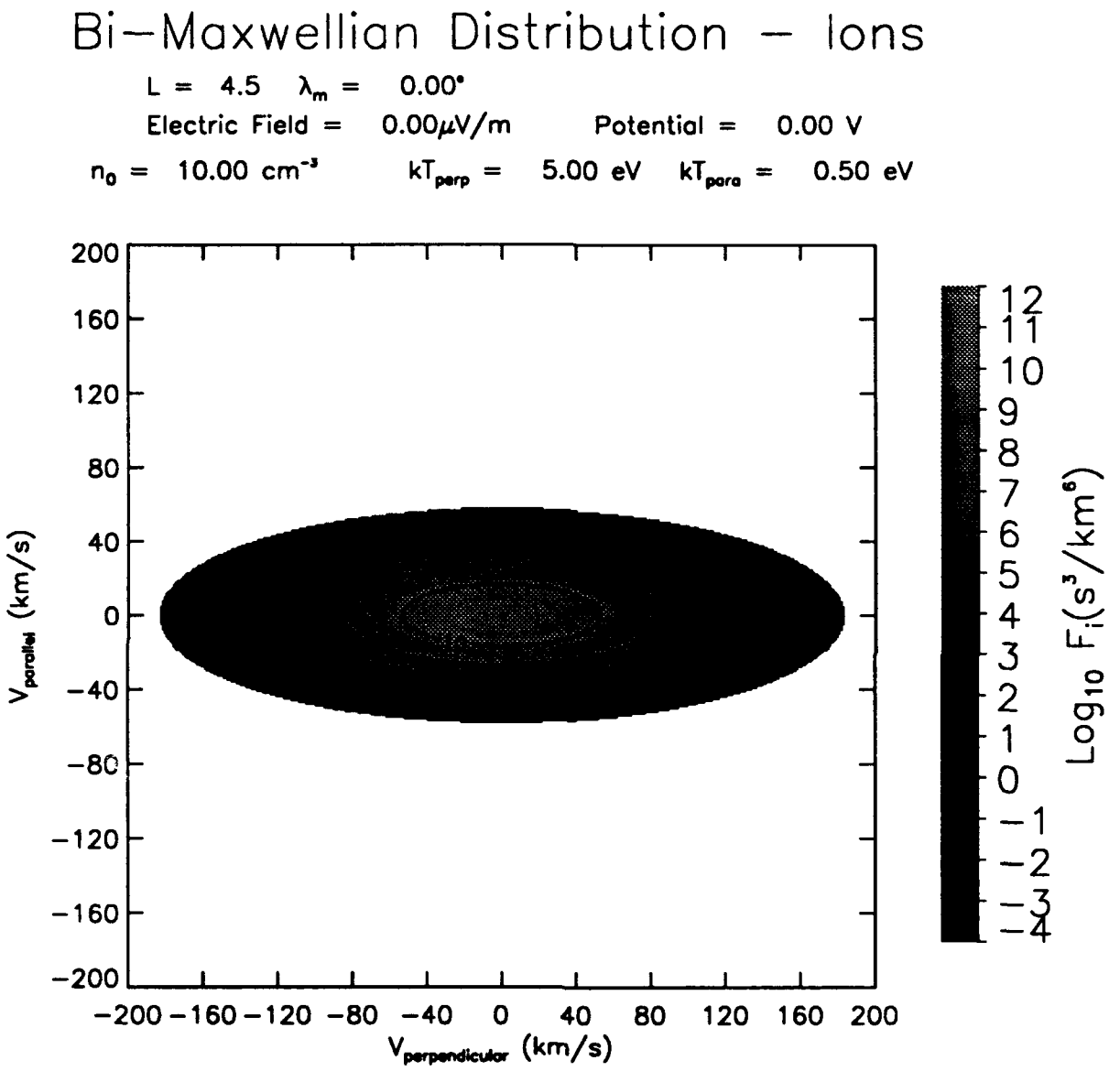

Figure 24. Bi-Maxwellian Distribution Function.

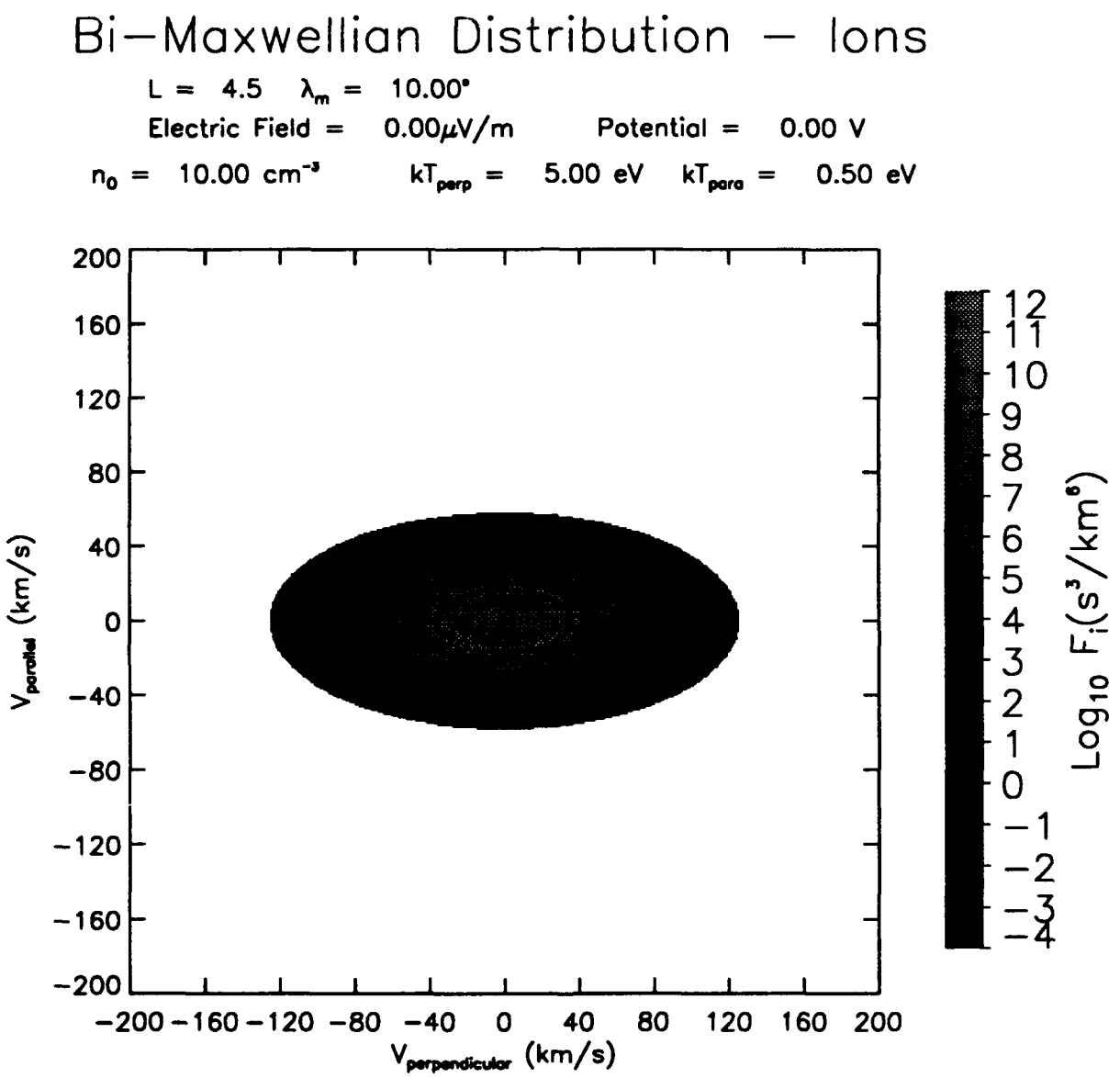

Figure 25. Bi-Maxwellian Distribution Function at $\lambda = 10^0$.

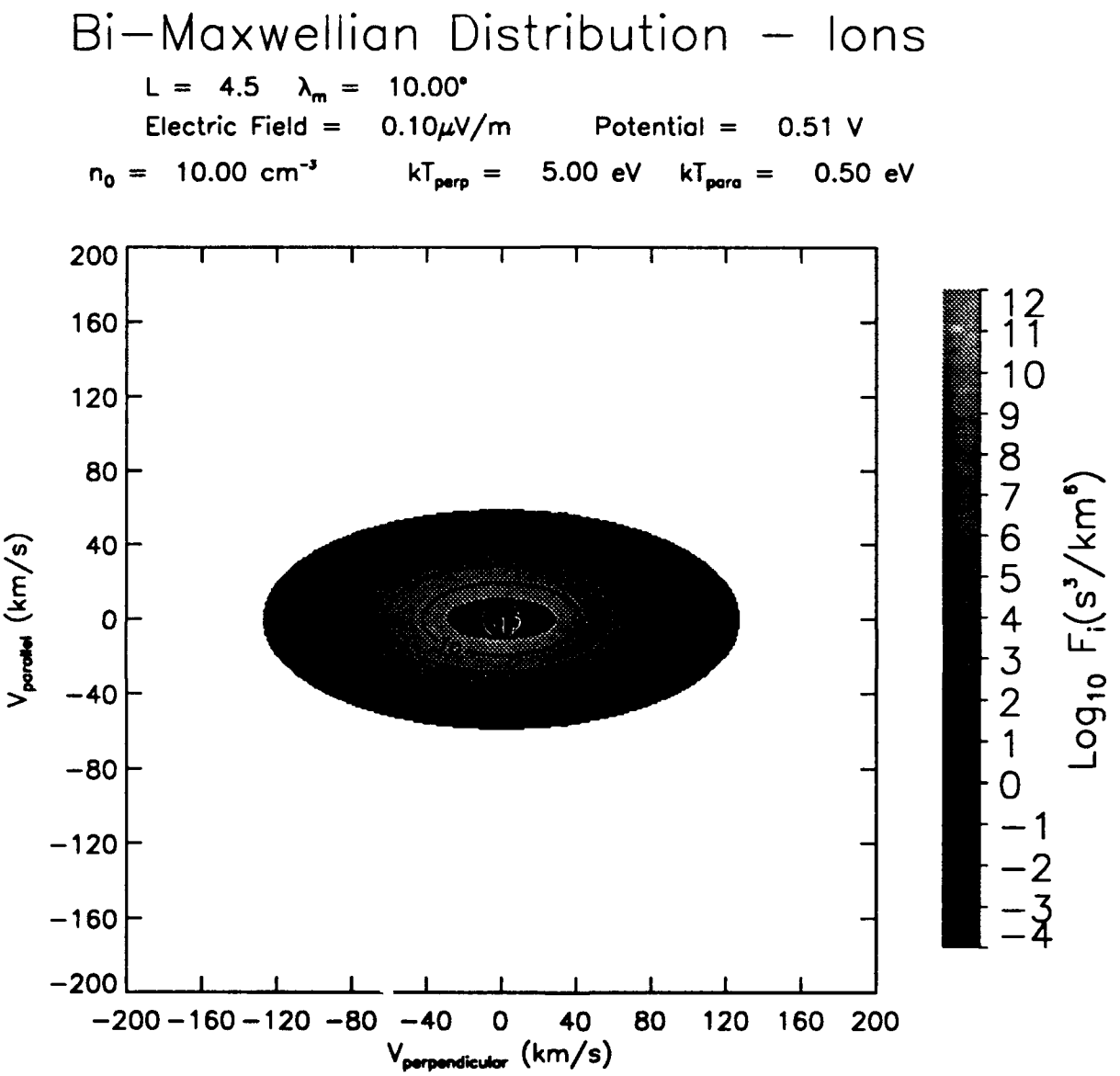

Figure 26. Bi-Maxwellian Distribution Function at $\lambda = 10^0$ (E = 0.1 μV/m).

function does not decrease as rapidly as when there is no electric field. This causes an increase in the density away from the equator. The density at $\lambda = 10^0$ when there is an electric field of 0.1 μV/m becomes 12.8 cm^{-3}. The consequence of a parallel electric field then is to exclude the low energy portion of the distribution for ions away from the magnetic equator which causes an increase in density off the equator. The region excluded by conservation of energy is the circular sector with the white circle with $mv^2/2 = q\phi$. Here $\phi = \int E ds$ = 0.5 V. The effect of a constant parallel electric field on density is shown in Figure 27. This result, coupled with previous observations (Fig. 15), motivates work to develop a model for self consistent electric fields.

B. SELF CONSISTENT ELECTRIC FIELD

The distributions shown thus far may be described as bi-Maxwellian with temperatures kT_{perp} = 10-50 eV and kT_{par} = 0.5-1.5 eV for ions, kT_{perp} = 27-250, and kT_{par} = 8-19 eV for electrons. In addition to the observed plasma distributions, it has been shown by Olsen [Ref. 10], that there is often cold isotropic plasma population that is "hidden" by the spacecraft potential. This cold isotropic background may comprise from 10-90% of the total density.

Persson [Ref. 11,12] has shown that an electric field parallel to the magnetic field must be present to ensure quasi neutrality when the pitch angle distributions for ions and electrons are different. The signature of parallel electric fields on observed particle distributions have been previously examined by Croley and others [Ref. 13,14]. Whipple [Ref. 15] has extended the theory of effects of parallel electric fields on particle distributions. He obtained an

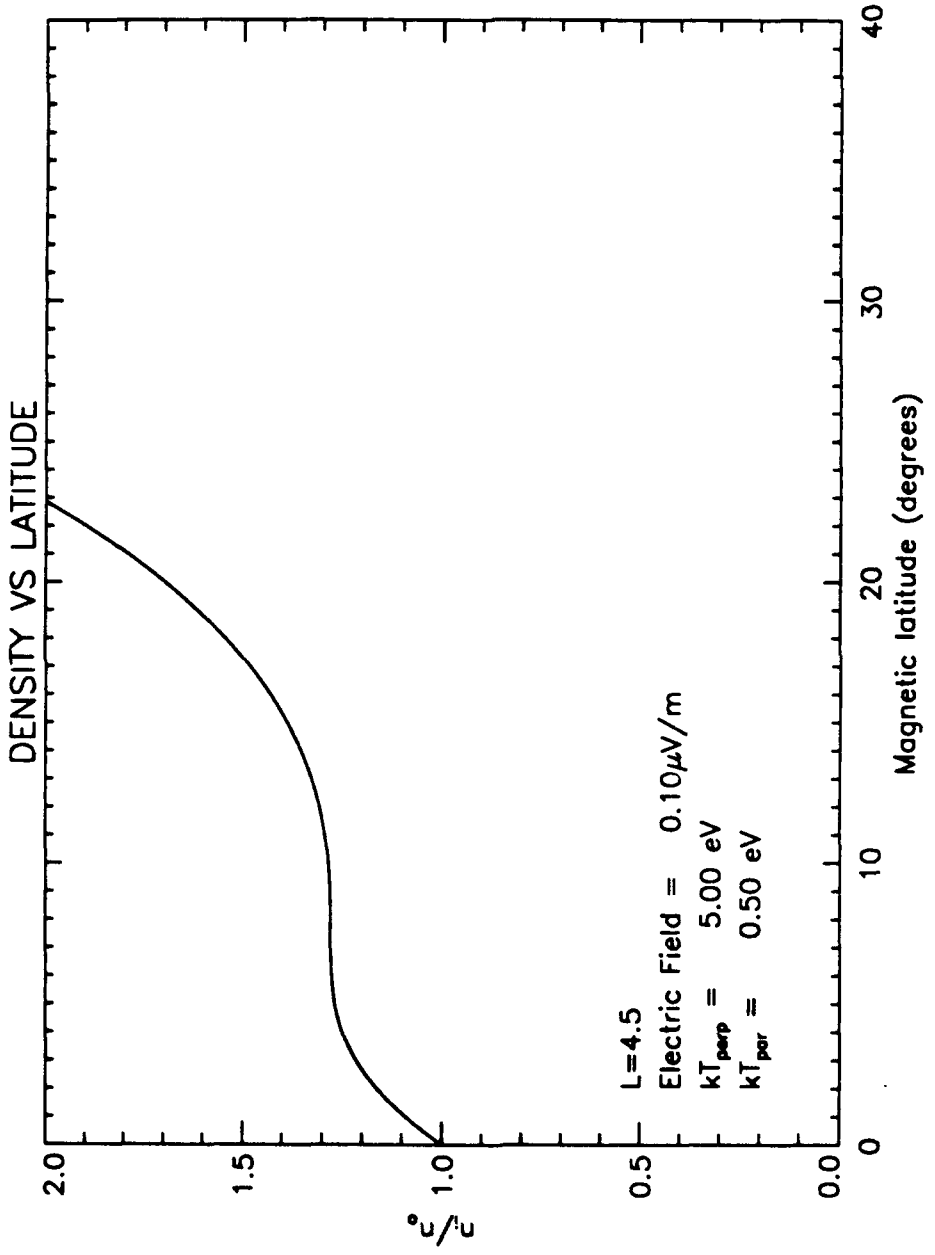

Figure 27. Density versus Magnetic Latitude (E=0.1 μV/m).

expression for the electric potential as a function of latitude for arbitrary distribution functions. This theoretical development is the basis for the work developed below.

The purpose of this section is to determine an expression for the electric field parallel to a magnetic field line, and the latidunal profile of the density, given that the equatorial distribution for ions is bi-Maxwellian, or a bi-Maxwellian superimposed upon a cold isotropic background, while the electron distribution is isotropic. The choice of plasma distributions is motivated by a desire to maintain reasonably analytic forms. Results from AMPTE [Ref. 16] indicate that there are regions where this approximation is valid. The solution will be derived for a steady state plasma where the density is so low that it may be considered to experience collisionless motion along a magnetic field line. The particle motion will be analyzed in terms of the conserved quantities along the magnetic field line, that is, the total Energy and the magnetic moment.

Whipple [Ref 15] has obtained the following expression for the species density for an arbitrary distribution function f:

$$n = \pi \frac{B}{2}\left[\frac{2}{m}\right]^{3/2} \int_{\mu=0}^{\infty} \int_{E=q\phi+\mu B}^{\infty} \frac{f^{+}+f^{-}}{\sqrt{E-q\phi-\mu B}}\, dE d\mu$$

where

$$E = \frac{m}{2}(v_{perp}^2+v_{par}^2)+q\phi(s) = \text{Total Energy}$$

$$\mu = \frac{mv_{perp}^2}{2B(s)} = \frac{mv^2\sin^2\alpha}{2B(s)} = \text{Magnetic moment}$$

$\phi(s)$ is the electrical potential as a function of the distance s along the magnetic field line, and f^{+} and f^{-} are the distribution functions for particles going in the positive ($ds/dt>0$) and negative ($ds/dt<0$) directions.

Liouvilles' theorem states that the distribution function for a collisionless plasma is constant along the particle trajectories. The distribution can be expressed entirely in terms of combinations of variables which remain constant. In this case, these constants are the invariants of the motion E and μ. Before performing the required integrations to obtain the density, the distribution function must first be converted from a function of velocities to a function of these invariants of the motion. Defining the electric potential, and density at the equator to be 0, and n_0, respectively, the distribution functions at the equator are:

$$f_{bi} = n_0\left[\frac{m}{2\pi kT_{perp}}\right]\left[\frac{m}{2\pi kT_{par}}\right]^{1/2} e^{-\left[\frac{\mu B_0}{kT_{perp}} + \frac{E-\mu B_0}{kT_{par}}\right]}$$

and

$$f_{iso}=n_0\left[\frac{m}{2\pi kT}\right]^{3/2} e^{-\frac{E}{kT}}.$$

Since equatorially trapped particles are being considered here it is expected that there will be symmetry between particles travelling in opposite directions, that is, $f^+ = f^- = f$, and this will be assumed for this model. Therefore

$$n = \pi B\left[\frac{2}{m}\right]^{3/2}\int_{\mu=0}^{\infty}\int_{E=q\phi+\mu B}^{\infty}\frac{f}{\sqrt{E-q\phi-\mu B}}dEd\mu.$$

If the bi-Maxwellian distribution function is now substituted into this equation the density is given by

$$\frac{n}{n_0} = \pi B\left[\frac{2}{m}\right]^{3/2}\left[\frac{m}{2\pi kT_{perp}}\right]\left[\frac{m}{2\pi kT_{par}}\right]^{1/2}\int_{\mu=0}^{\infty}\int_{E=q\phi+\mu B}^{\infty}\frac{e^{-\left[\frac{\mu B_0}{kT_{perp}}+\frac{E-\mu B_0}{kT_{par}}\right]}}{\sqrt{E-q\phi-\mu B}}dEd\mu$$

and a straightforward integration yields

$$\frac{n}{n_0} = \frac{e^{-\frac{q\phi}{kT_{par}}}}{1-\gamma} \tag{1}$$

where

$$\gamma = \left[1-\frac{B_0}{B}\right]\left[1-\frac{kT_{perp}}{kT_{par}}\right].$$

For an isotropic distribution

$$\frac{n}{n_0} = e^{-\frac{q\phi}{kT}}. \tag{2}$$

1. Bi-Maxwellian Ions and Isotropic electrons

If the condition of quasi neutrality is now invoked the electric potential may be solved for as a function of the distance s along the magnetic field line. Using subscripts i and e for ions and electrons, and assuming that Hydrogen is the only species of ions present, we now have

$$\frac{e^{-\frac{e\phi}{kT_{par_i}}}}{1-\gamma_i} = e^{\frac{e\phi}{kT_e}}.$$

Solving for ϕ

$$\phi = -\frac{1}{e\left[\frac{1}{kT_{par_i}}+\frac{1}{kT_e}\right]}\ln(1-\gamma_i) \tag{3}$$

Figure 28 shows this potential plotted as a function of magnetic latitude for several ratios of kT_{perp} to kT_{par}. The potential is a maximum at the equator, with larger anisotropy ratios leading to a steeper slope.

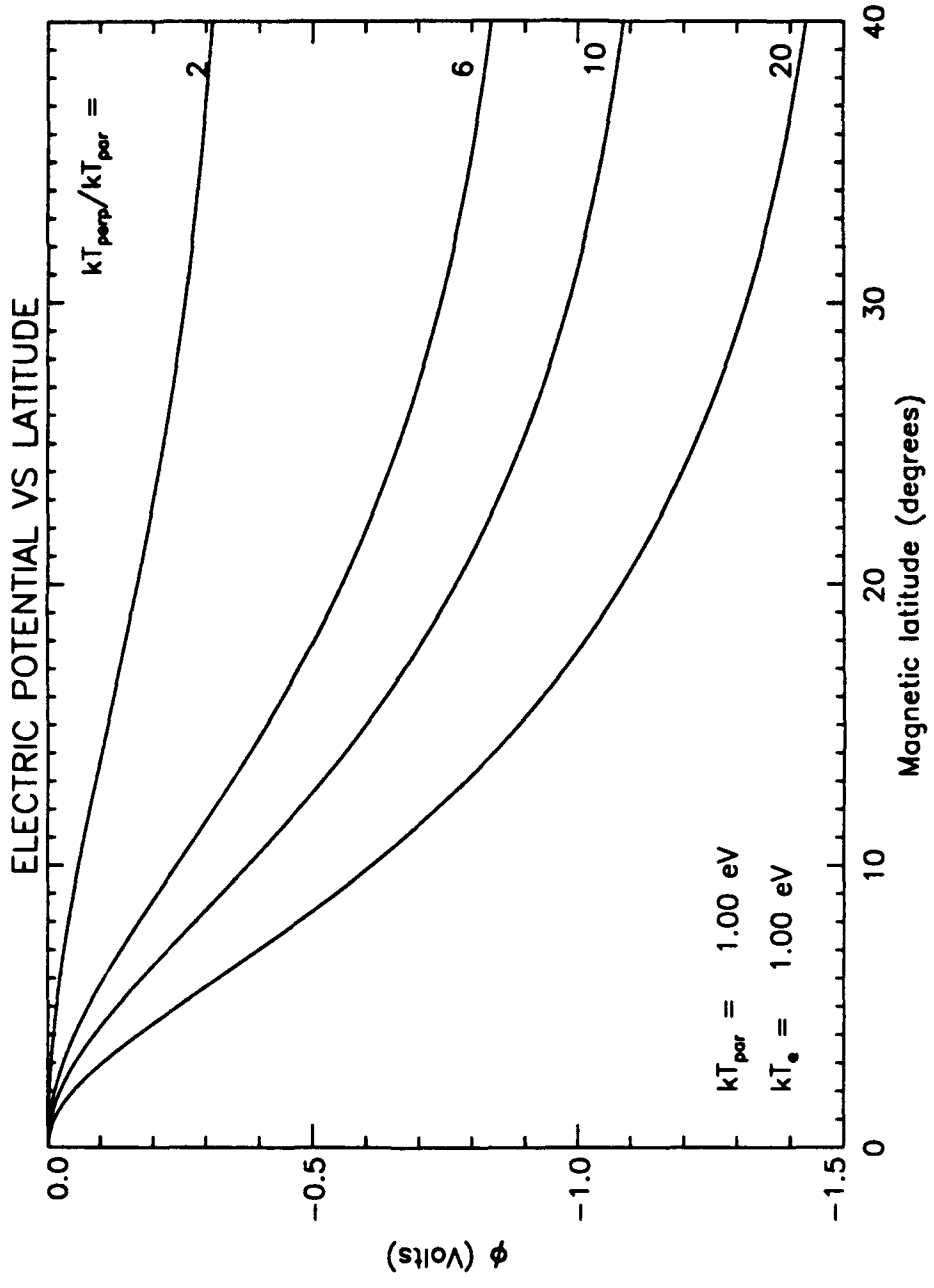

Figure 28. Electric Potential as a function of Magnetic Latitude.

The parallel electric field may now be obtained by taking the gradient of ϕ.

$$\vec{E} = -\nabla\phi(s) = -\frac{\partial\phi(s)}{\partial s}\hat{s}$$

from which we obtain

$$\vec{E} = -\frac{3\left[1-\frac{kT_{perp_i}}{kT_{par_i}}\right]\cos^4\lambda\sin\lambda\left[3+5\sin^2\lambda\right]}{LR_E e\left[\frac{1}{kT_{par_i}}+\frac{1}{kT_e}\right]\left[1-\gamma_i\right]\left[1+3\sin^2\lambda\right]^2}\hat{s}.$$

The magnitude of the electric field as a function of latitude is shown in Figure 29. The strength of the electric field is related to the degree of anisotropy with greater anisotropy leading to stronger electric fields. The strength of the electric field is on the order of 0.1 μV/m.

The density profile may also be obtained by substituting the expression for ϕ (3) into (1), which after rearranging gives

$$\frac{n_i}{n_0} = (1-\gamma_i)^{\left[\frac{1}{1+\frac{kT_{par_i}}{kT_e}}\right]-1}.$$

This density profile is shown in Figure 30, from which we see that the density is a maximum at the equator. This is the effect of particles trapped in a magnetic mirror. Greater anisotropy confines the particles closer to the equator. This result for a self consistent electric field differ from that for a constant electric field, and gives the opposite trend in the density profile. In a sense, this is contrary to our goal. Partly for this reason, we continue by looking at the consequences of adding an isotropic background.

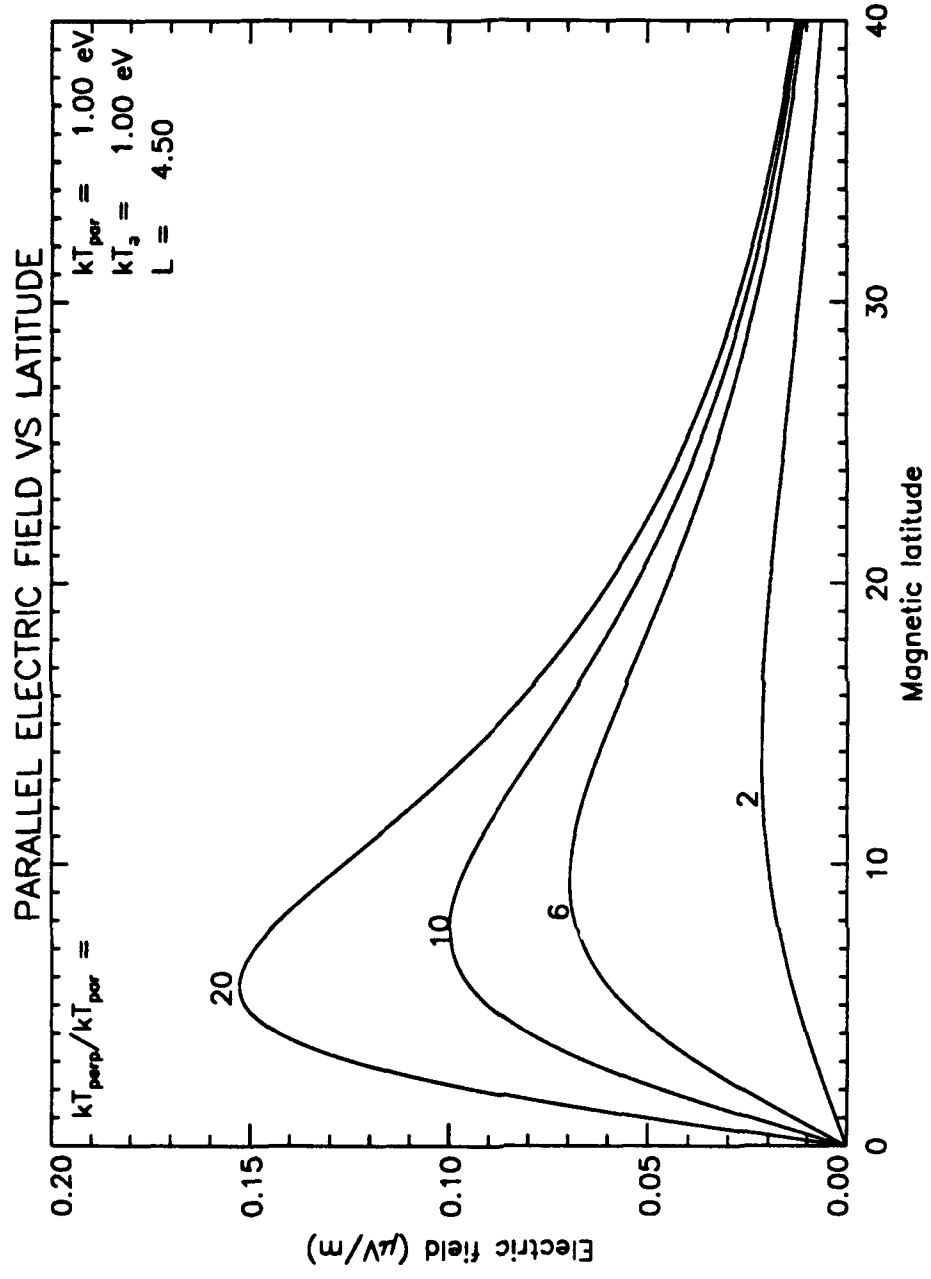

Figure 29. Parallel Electric Field as a function of Magnetic Latitude.

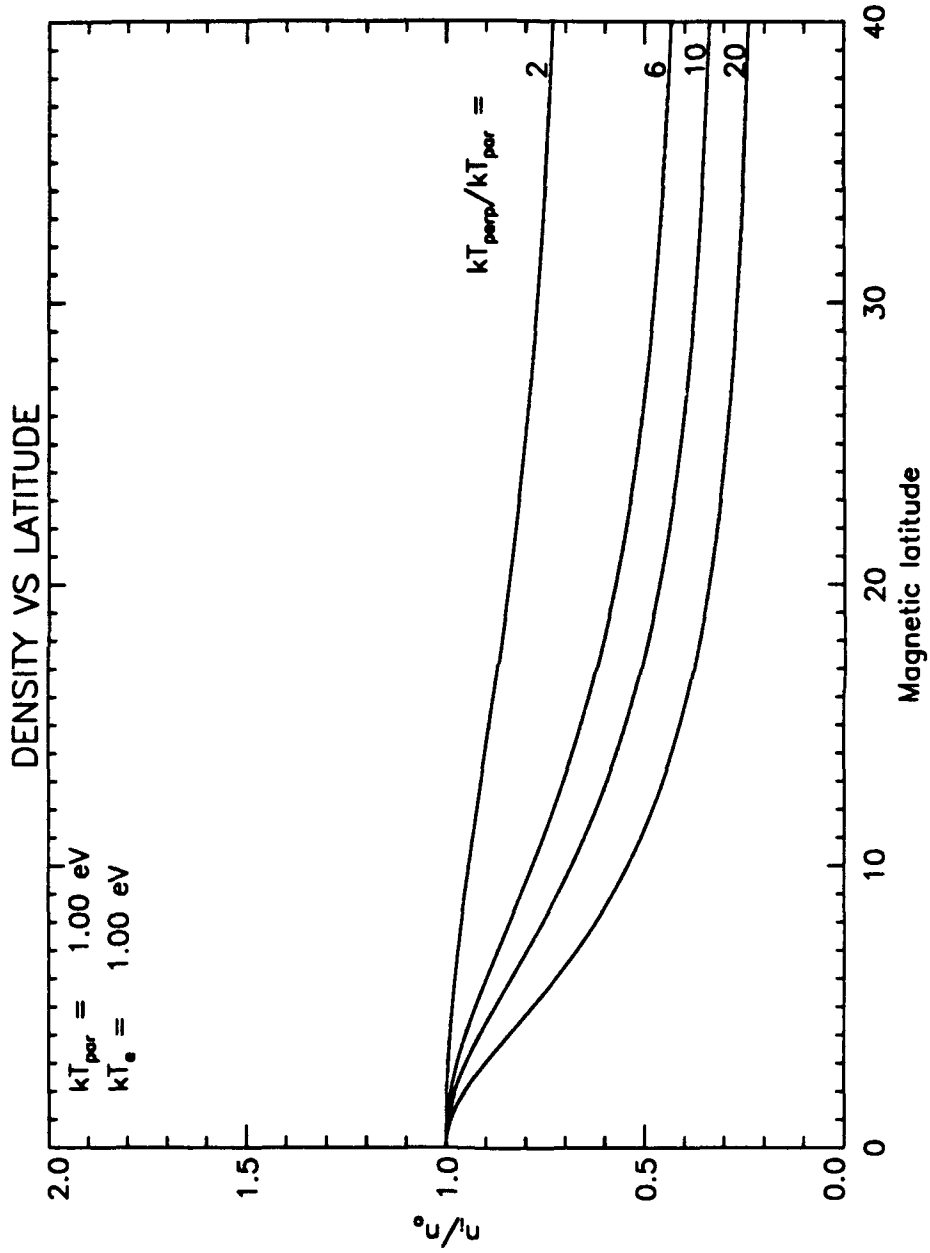

Figure 30. Density as a function of Magnetic Latitude.

2. Bi-Maxwellian and Isotropic Ions, Isotropic electrons

If we add an isotropic ion background and assume that the isotropic ion temperature is equal to the parallel temperature of the ions (≈1 eV), which is reasonable, the ion and electron density profiles are then given by

$$\frac{n_i}{n_0} = e^{-\frac{e\phi}{kT_{par_i}}}\left[R+\frac{1-R}{1-\gamma_i}\right] \tag{4}$$

$$\frac{n_e}{n_0} = e^{\frac{e\phi}{kT_e}}$$

where R is the ratio of the isotropic to the total ion density. Invoking the condition of quasi neutrality yields

$$e^{-\frac{e\phi}{kT_{par_i}}}\left[R+\frac{1-R}{1-\gamma_i}\right] = e^{\frac{e\phi}{kT_e}}.$$

Solving for ϕ, the result is

$$\phi = -\frac{kT_{par_i}}{e}\ln\left[R+\frac{1-R}{1-\gamma_i}\right]^{-\frac{1}{\left[1+\frac{kT_{par_i}}{kT_e}\right]}} \tag{5}$$

which upon differentiating to obtain the electric field is

$$\vec{E} = -\frac{3kT_{par_i}\left[1-R\right]\left[1-\frac{kT_{perp_i}}{kT_{par_i}}\right]\cos^4\lambda\sin\lambda\left[3+5\sin^2\lambda\right]}{el.R_E\left[1+\frac{kT_{par_i}}{kT_e}\right]\left[1-\gamma_i\right]^2\left[R+\frac{1-R}{1-\gamma_i}\right]\left[1+3\sin^2\lambda\right]^2}\hat{s}.$$

The density profile is again obtained by substituting for ϕ in equation (5) into (4) to obtain

$$\frac{n_i}{n_0} = \left[R + \frac{1-R}{1-\gamma_i}\right]^{1-\frac{1}{\left[1+\frac{kT_{par_i}}{kT_e}\right]}}.$$

Figures 31, 32 and 33 are plots of the electric potential, the magnitude of the electric field and density profiles as a function of magnetic latitude. The results are plotted for ratios of the isotropic to total ion density from 10 to 90 percent. The results are similar to those for a purely bi-Maxwellian ion distribution. The isotropic component has the effect of lessening the effect of the anisotropic distribution. The density and potential do not decrease as rapidly as latitude increases, and the strength of the electric field is decreased. There are not, however any qualitative changes in the shapes of the electric field, potential, or density distributions.

C. COMPARISON OF OBSERVATIONS TO MODEL #2

Figure 34 is a plot of the density profile as observed by the DE-1 satellite on day 315. The density has been normalized by the factor $(L/4.5)^{-4}$ to eliminate the radial dependence, introduced by the satellite orbit, from the density profile. The dashed line is the density profile which is predicted by the model for temperatures and density determined from the fit to the distribution shown in Figure 22. These are kT_{perp} = 20 eV, kT_{par} = 2.5 eV, and a total density of 40 cm^{-3} and the density of the bi-Maxwellian component is 30 cm^{-3}.

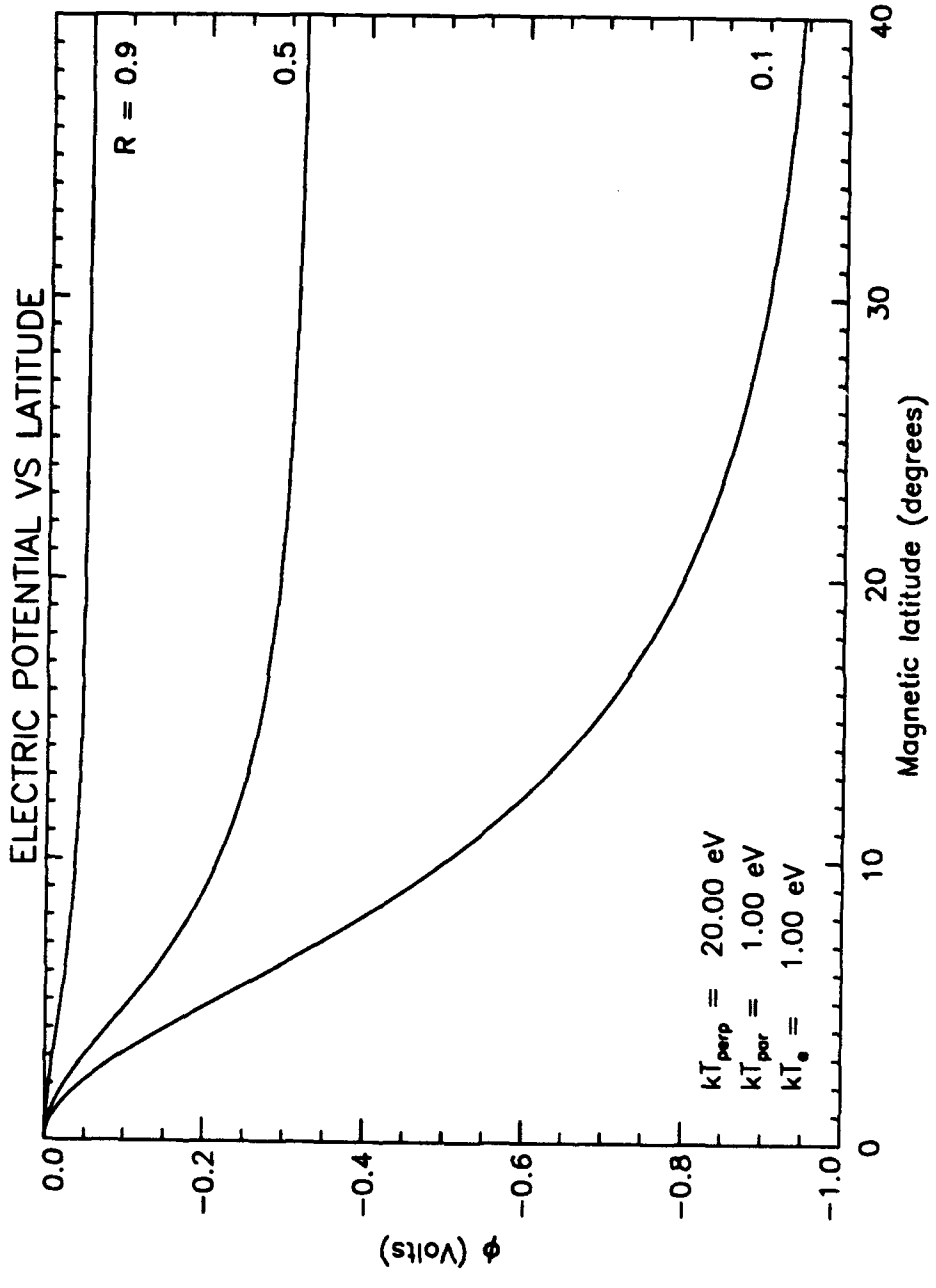

Figure 31. Electric Potential as a function of Magnetic Latitude.

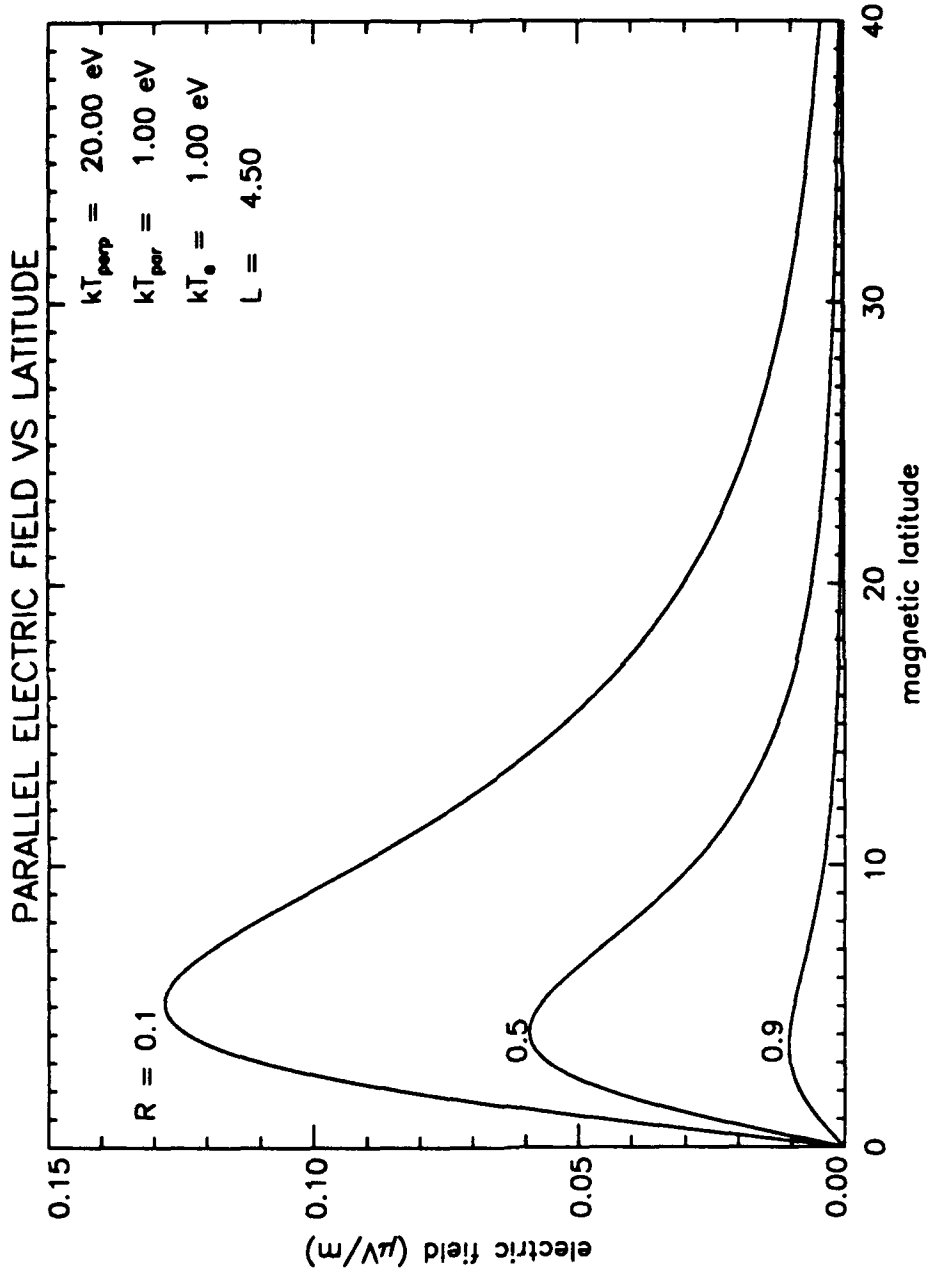

Figure 32. Parallel Electric Field as a function of Magnetic Latitude.

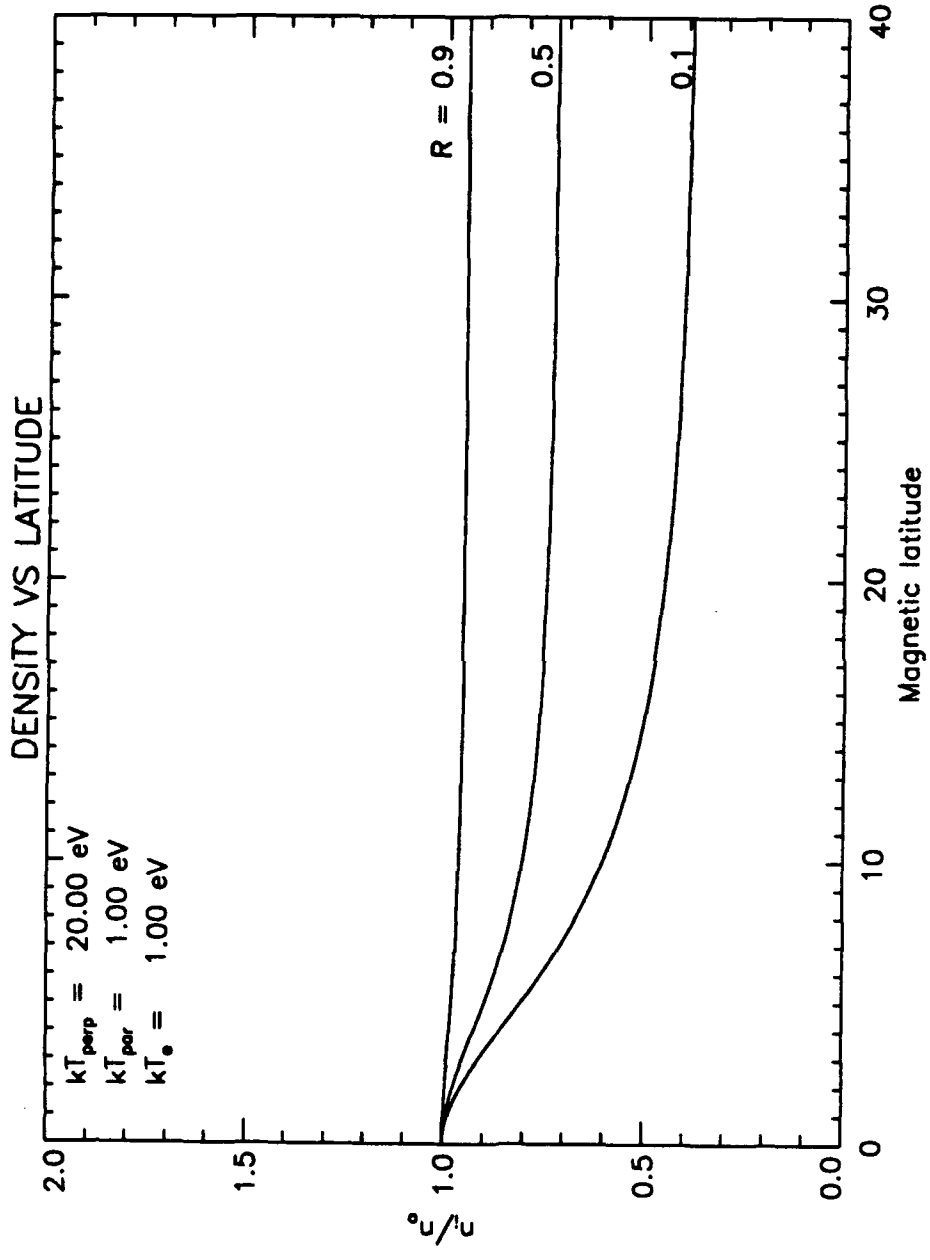

Figure 33. Density as a function of Magnetic Latitude.

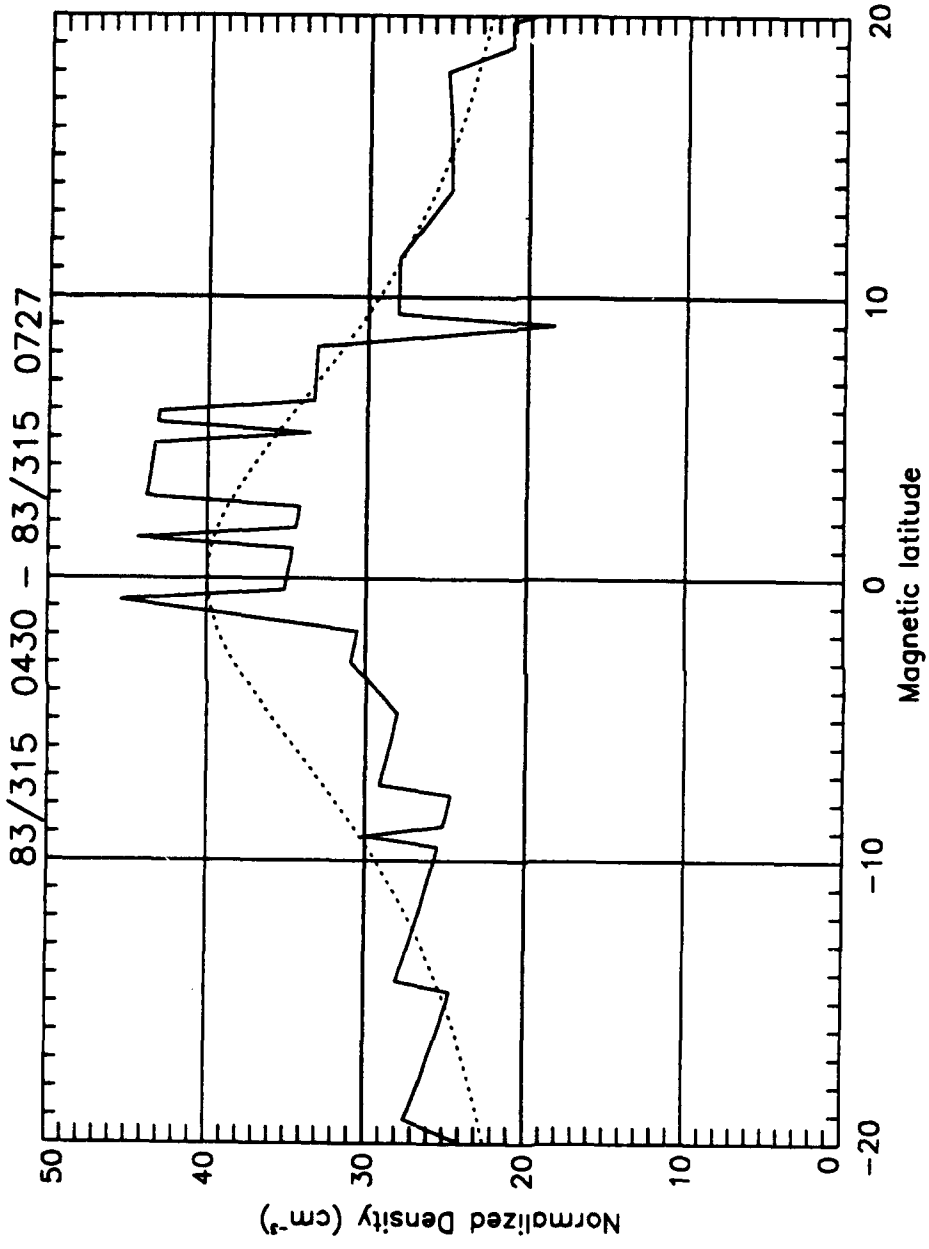

Figure 34. Density as a function of Magnetic Latitude, DE-1 Day 315 of 1983.

The observed profile is consistent with the predicted results. This agreement is obtained without any free parameters, aside from the assumption that the electron distribution is isotropic.

Other measurements of the density profile have shown that there is more typically a density minimum at the magnetic equator, in apparent contradiction with the predicted results. A characteristic density minimum profile is that where the density is approximately constant between $\lambda = -10^0$ to 10^0, at which latitudes it abruptly increases [Ref. 12]. In such cases, the density approximately doubles over 1 degree of latitude. Such a density profile is shown in Figure 35. Instead of invoking the condition of quasi neutrality to determine the electric potential and parallel electric field, the potential may be solved for by substituting the given ion density profile into equation (4). The resultant electric potential and field is shown in Figures 36 and 37. Now that the potential is known the electron density profile may be solved for. If the electrons are still assumed to be isotropic the electron density profile is given by equation (3). Figure 38 is a plot of the given ion density profile and the electron density profile that results. There is a relatively large difference in the ion and electron densities away from the equator. The difference in the density profiles increases with greater anisotropy ratios for the ions. This is in clear violation of the principle of quasi neutrality of plasmas.

A possible explanation of this is that when a density minimum is observed, the electrons are not described by an isotropic distribution, but by a bi-Maxwellian with a parallel temperature that is greater than the perpendicular temperature, that is, the electrons are field aligned. One example of a field aligned distribution is seen by the SCATHA satellite on Day 179 of 1979.

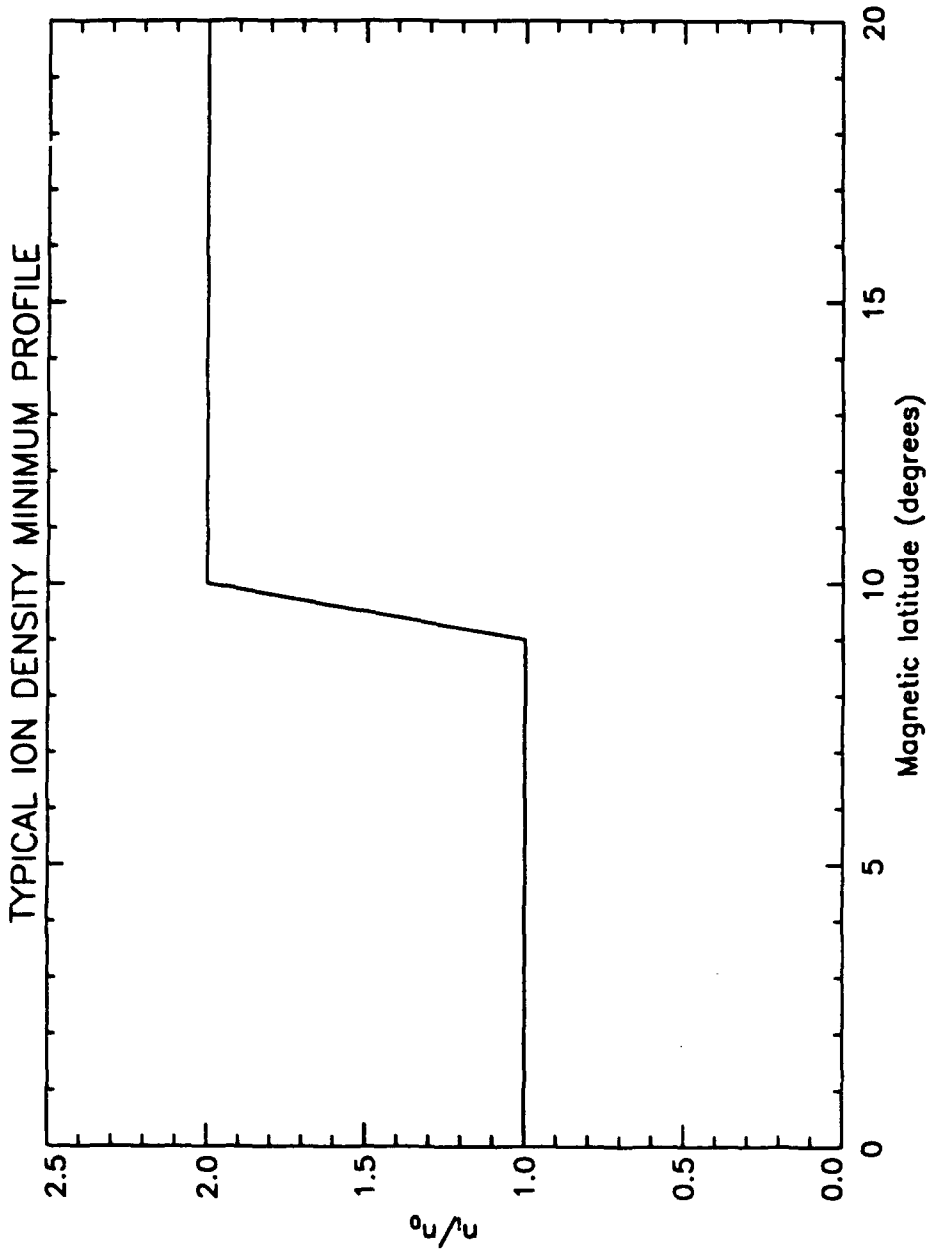

Figure 35. Typical Ion Density Minimum Profile.

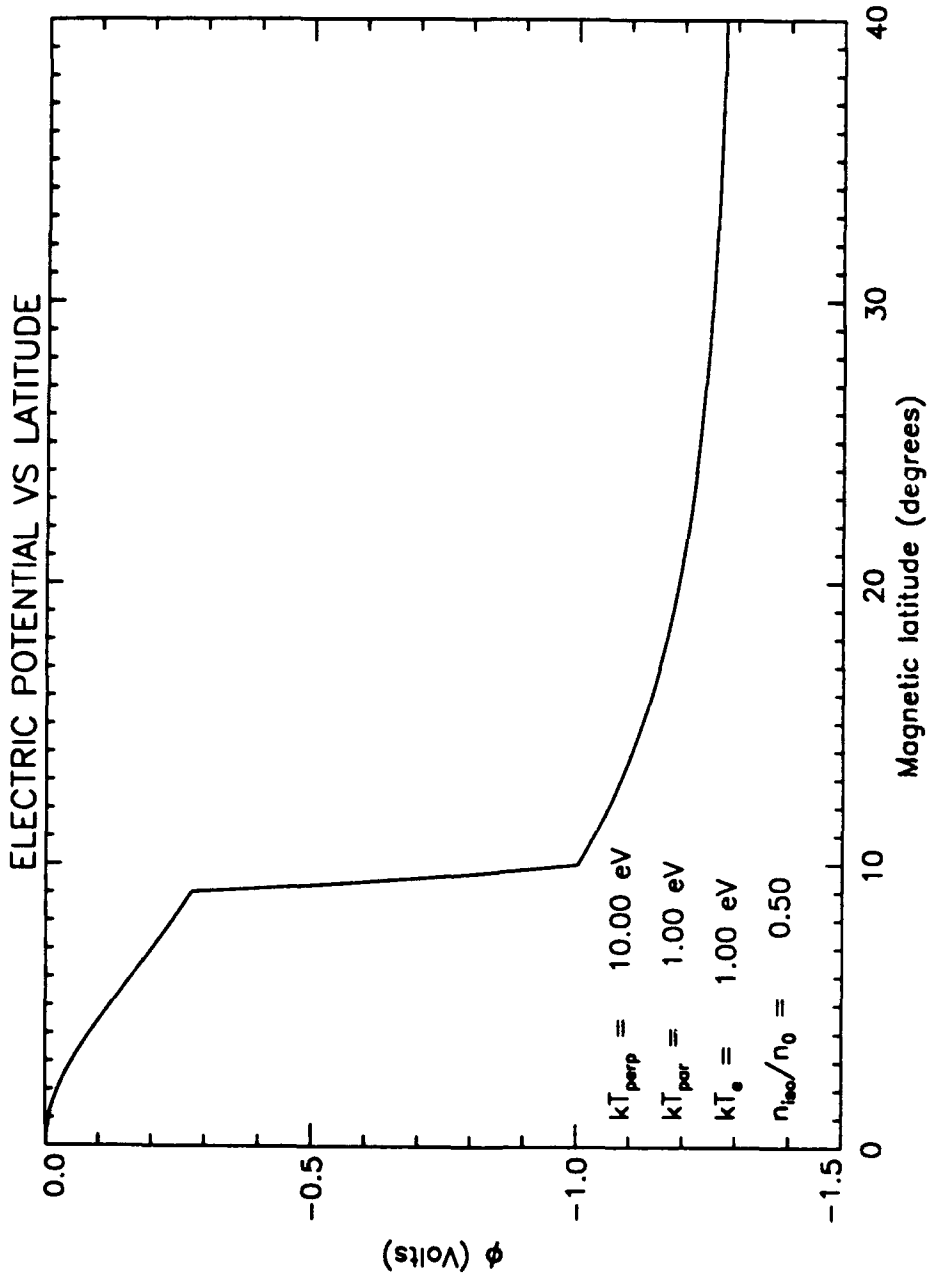

Figure 36. Electric Potential as a function of Magnetic Latitude.

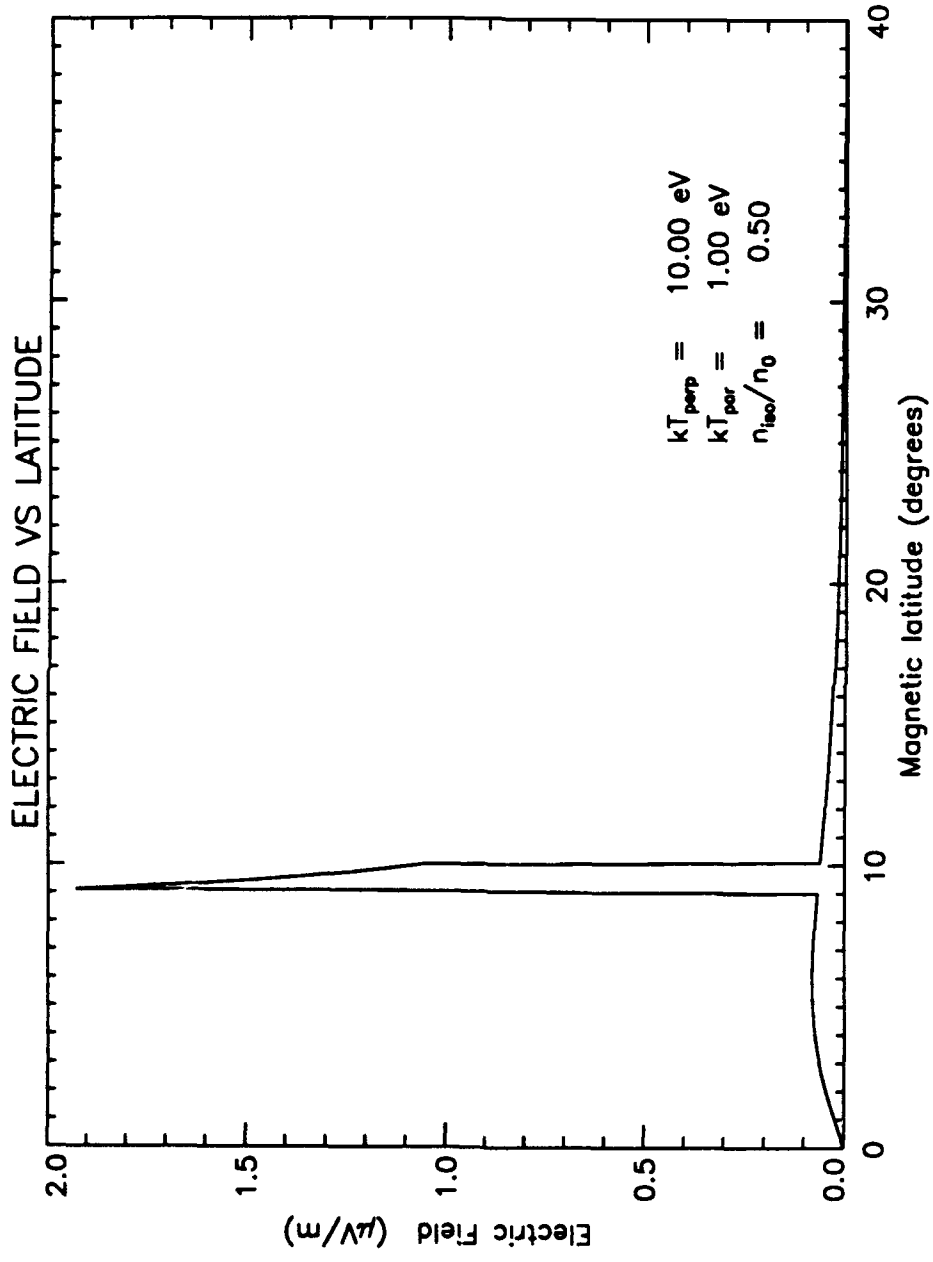

Figure 37. Electric Field as a function of Magnetic Latitude.

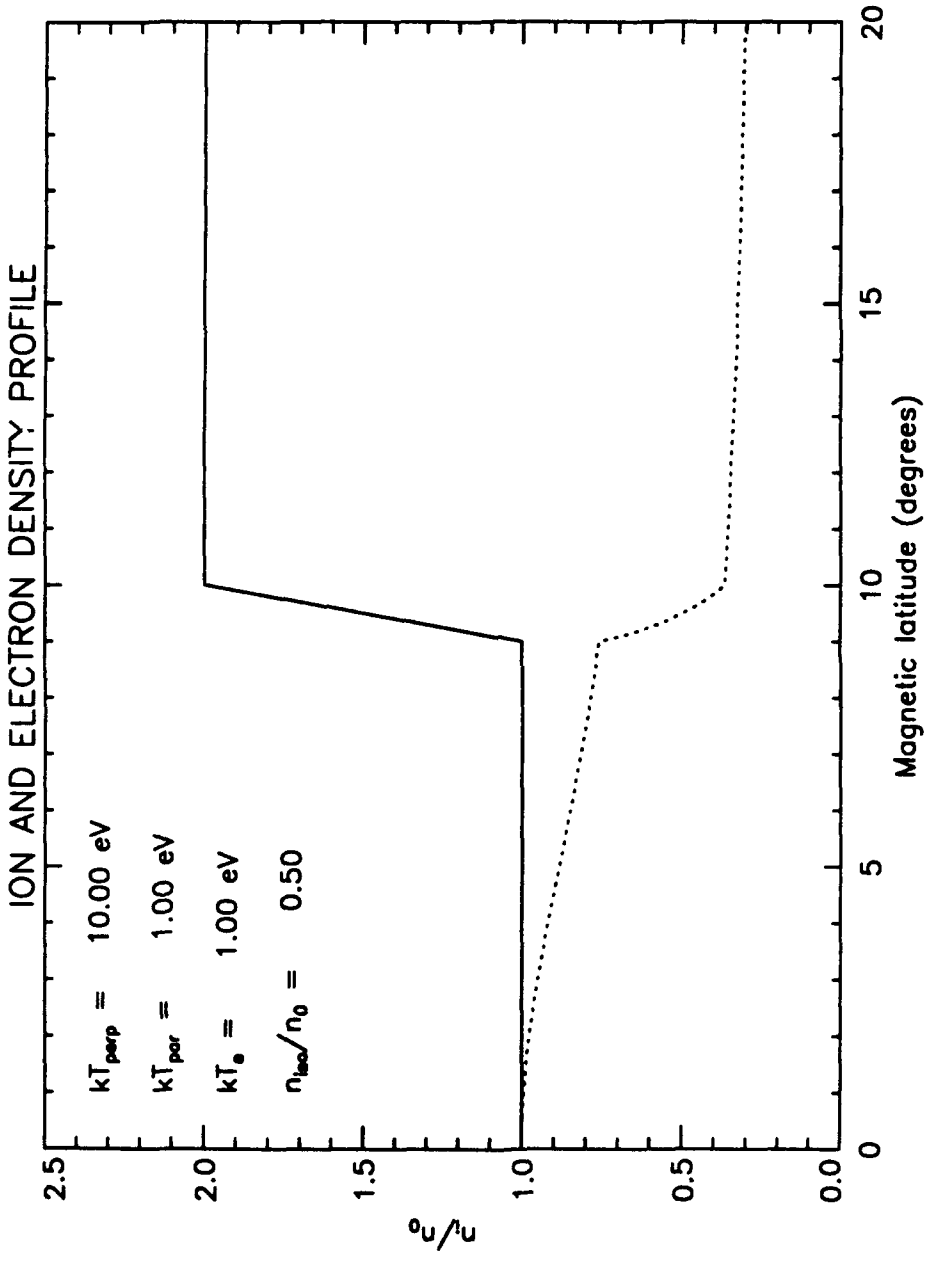

Figure 38. Ion and Electron Density as a function of Magnetic Latitude.

The pitch angle distribution for the field aligned portion of the electron distribution is shown in Figure 39. The $\log_{10} f$ is plotted against $\cos^2\alpha$, for low pitch angles. The bi-Maxwellian fit to this portion of the distribution gives for the temperatures kT_{perp}=2.6 and kT_{par}=21 eV. When these values are used in the determination of the density profile, the result is shown in Figure 40. The dashed line in this figure is the electron density profile for the given ion density profile. There is good agreement between the ion and electron densities up to $\lambda \approx 10^0$. Beyond this latitude the analysis is invalid because the ion and electron distributions are no longer described by a bi-Maxwellian. These results imply that the density minimum that is observed is associated with field aligned electron distributions.

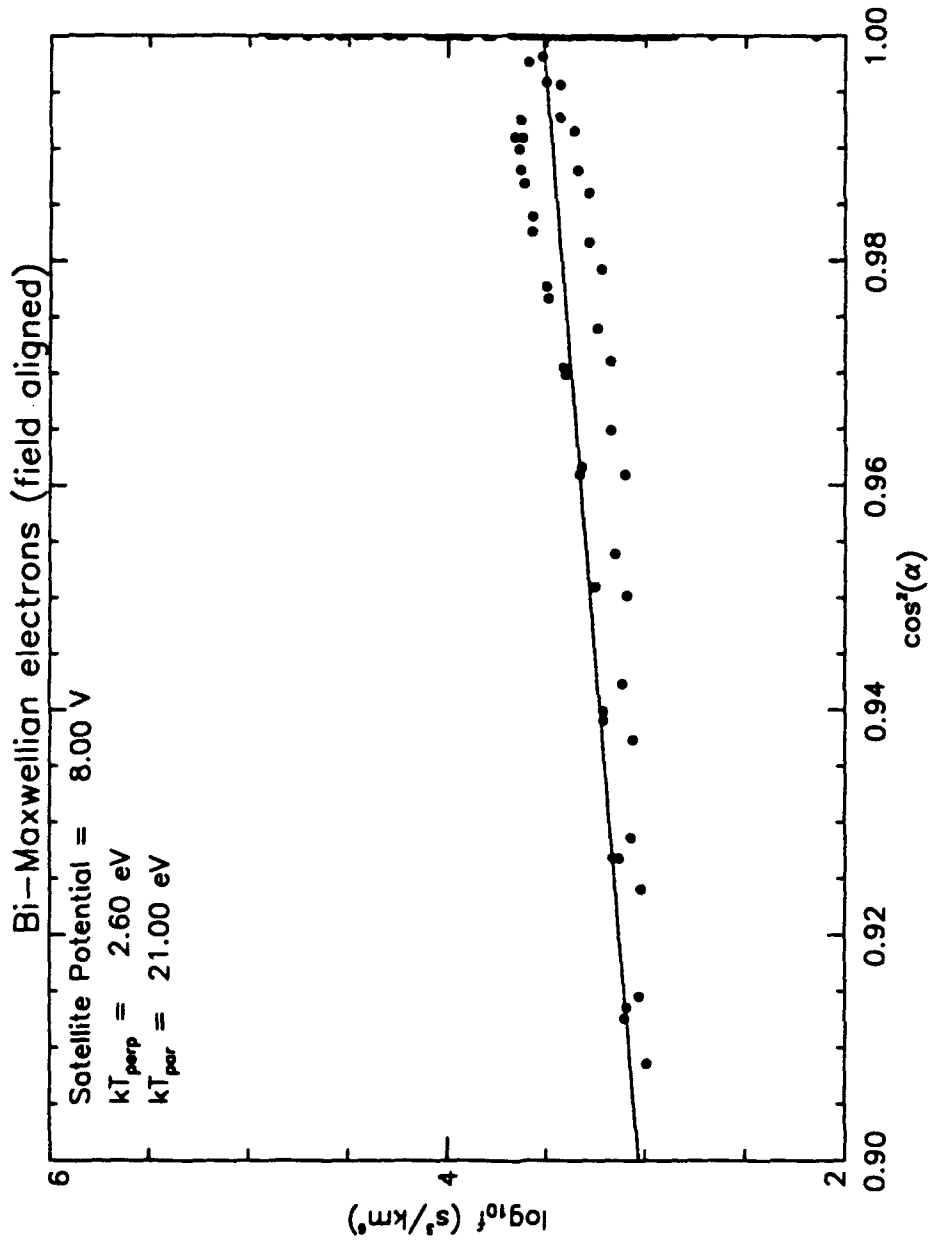

Figure 39. Electron Field Aligned Distribution, SCATHA Day 179 of 1979.

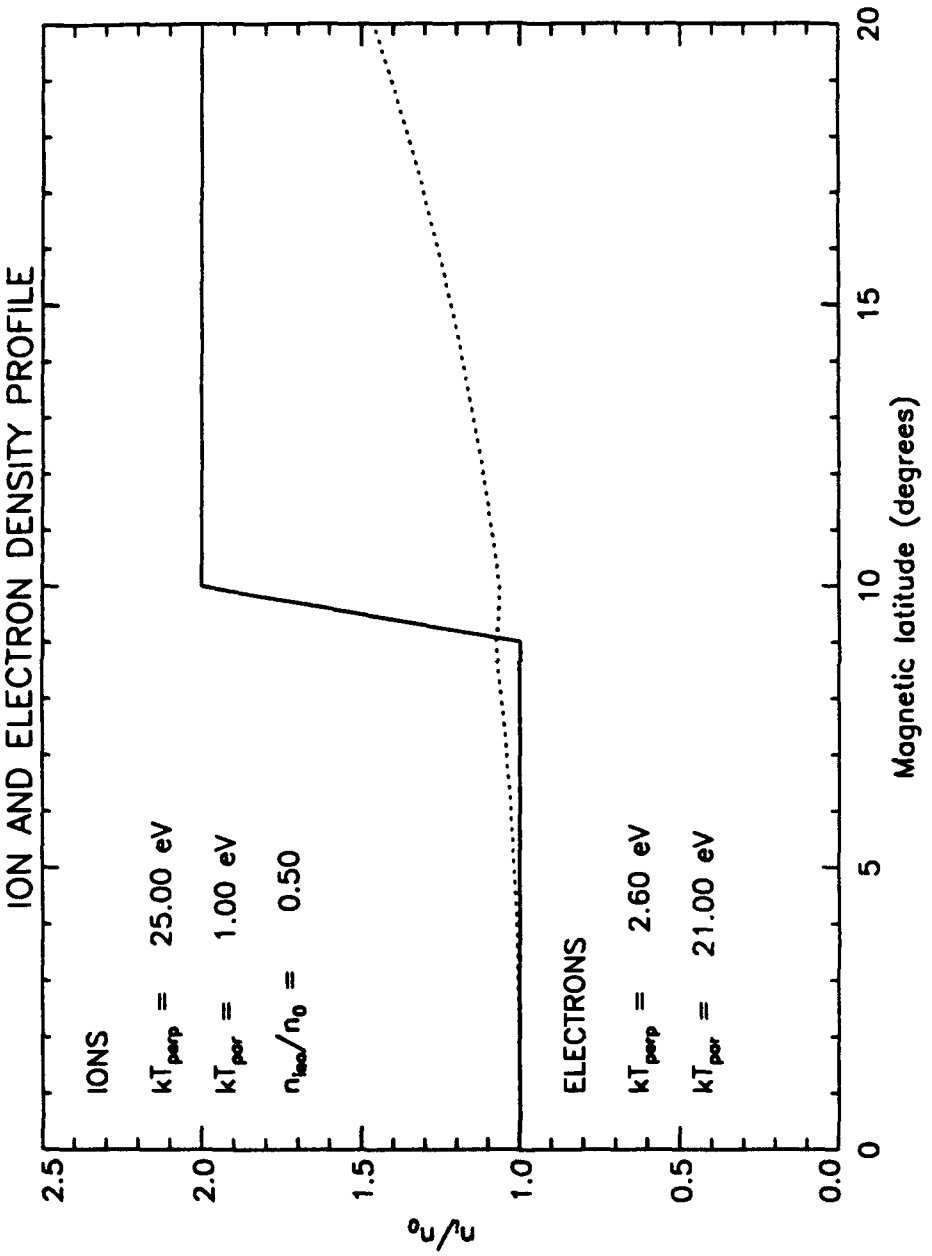

Figure 40. Ion and Electron Density Profile (electrons field aligned).

V. CONCLUSIONS

It has been shown that equatorially trapped plasmas may be described by a bi-Maxwellian distribution function. The consequence of this distribution is that an electric field parallel to the magnetic field must result in order to preserve quasi neutrality. The strength of the electric field that results is on the order of 0.1μV/m. The density profile that results from this distribution is a maximum at the equator with greater anisotropy confining the particles closer to the equator. The effect of the electric field is to reduce the amount by which the density decreases. A comparison of the observed density profile to the density profile predicted by the model, shown in Figure 34, shows good agreement.

Data have also shown that a density minimum sometimes exists at the magnetic equator with an abrupt increase in density at approximately $\pm 10^0$ in latitude where the density approximately doubles. If the density profile is given the electric potential, and hence the electric field, may be calculated. The results for the potential and strength of the electric field are similar to the solution when quasi neutrality was assumed, with the exception that the gradient in potential and strength of the electric field are very large at the boundary where the density abruptly increases. The calculated electron density profile shows that the condition of quasi neutrality is violated if the electrons are assumed to be isotropic. If the electrons are instead field aligned, quasi neutrality is preserved up to the boundary in the ion density profile. This implies the presence of a field aligned electron distribution whenever a density minimum is observed at the equator.

LIST OF REFERENCES

1. Halliday, D., and Resnick, R., *Fundamentals of Physics,* 3rd ed., p. 598, John Wiley & Sons, Inc., 1988.

2. Parks, G. K., *Physics of Space Plasmas,* pp. 21-24,55, Addison-Wesley Publishing Company, 1991.

3. Chen, F. F., *Introduction to Plasma Physics and Controlled Fusion,* 2nd ed., v. 1, Plenum Press, 1983.

4. DeForest, S. E., and others, *Handbook for UCSD SC9 SCATHA Auroral Particles Experiment,* University of California at San Diego, Revised edition, 1980.

5. Olsen, R. C., "Equatorially Trapped Plasma Populations", *Journal of Geophysical Research,* v. 86, pp. 11235-11245, 1 December 1981.

6. Hoffman R. A., and others, *Dynamics Explorer,* pp. 477-499, D. Reidel Publishing Company, 1981.

7. National Aeronautics and Space Administration Report NASA TM-82484, *Instrument Manual for the Retarding Ion Mass Spectrometer on Dynamics Explorer-1,* by S. A. Fields, and others, pp. 1-5, 33-41, May 1982.

8. Olsen, R. C., and others, "Plasma Observations at the Earth's Magnetic Equator", *Journal of Geophysical Research,* v. 92, pp. 2385-2407, 1 March 1987.

9. Olsen, R. C., "The Density Minimum at the Earth's Magnetic Equator", in press, *Journal of Geophysical Research,* 1991.

10. Olsen, R. C., and others, "The Hidden Ion Population: Revisited", *Journal of Geophysical Research,* v. 92, pp. 2385-2407, 1 December 1985.

11. Persson, H., "Electric Field along a Magnetic Line of Force in a Low-Density Plasmaa", *The Physics of Fluids,* v. 6, pp. 1756-1759, December 1963.

12. Persson, H., "Electric Field Parallel to the Magnetic Field in a Low-Density Plasma", *The Physics of Fluids,* v. 9, pp. 1090-1098, 1966.

13. Croley, D. R., and others, "Signature of a Parallel Electric Field in Ion and Electron Distributions in Velocity Space", *Journal of Geophysical Research,* v. 83, pp. 2701-2705, 1 June 1978.

14. Mizera, P. F., and Fen..ell, J. F., "Signatures of Electric Fields From High and Low Altitude Particles Distributions", *Geophysical Research Letters,* v. 4, pp. 311-314, August 1977.

15. Whipple, E. C., "The Signature of Parallel Electric Fields in a Collisionless Plasma", *Journal of Geophysical Research,* v. 82, pp. 1525-1530, 1 April 1977.

16. Braccio, P. G. *Survey of Trapped Plasmas at the Earth's Magnetic Equator,* Master's Thesis, Naval Postgraduate School, Monterey, California, December 1991.

INITIAL DISTRIBUTION LIST

1.	Defense Technical Information Center Cameron Station Alexandria, Virginia 22304-6145	2
2.	Library, Code 52 Naval Postgraduate School Monterey, California 93943-5002	2
3.	Professor K. E. Woehler, Code PH/Wh Chairman, Department of Physics Naval Postgraduate School Monterey, California 93943-5000	2
4.	Dr. R. C. Olsen, Code PH/0S Department of Physics Naval Postgraduate School Monterey, California 93943-5000	2
5.	LT P. G. Braccio 10 Brookside Dr. Greenwich, Connecticut 06830	1
6.	Dr. E. C. Whipple NASA/HQ/SS Washington DC 20546	1
7.	Dr. T. E. Moore NASA/MSFC/ES53 Huntsville, Alabama 35812	1
8.	Dr. J. L. Horwitz CSPAR University of Alabama Huntsville, Alabama 35899	1
9.	Dr. N. Singh Department of Electrical Engineering University of Alabama Huntsville, Alabama 35899	1
10.	Mr. G. Joiner, Code 11/4SP Office of Naval Research 800 N. Quincy St. Arlington, Virginia 22217	1

11. LT L. J. Scott
3805 Eunice Hwy.
Hobbs, New Mexico 88240 1